1970

Progress report on fracture toughness of structural steels, May 1970

G. R. Irwin

K. J. Pietrzak

DYNAMIC FRACTURE TOUGHNESS OF STRUCTURAL STEELS

by

Kenneth Pietrzak

A Thesis

Presented to the Graduate Committee

of Lehigh University

in Candidacy for the Degree of

Master of Science

in

Civil Engineering

Lehigh University

1971

This thesis is accepted and approved in partial fulfillment of the requirements for the degree of Master of Science in Civil Engineering.

18 May 1971

Dr. George R. Irwin

Dr. D. A. VanHorn, Chairman
Department of Civil Engineering

TABLE OF CONTENTS

TABLE OF CONTENTS (continued)

LIST OF FIGURES

LIST OF FIGURES (continued)

ABSTRACT

This report presents mainly the work done on Project 366, the "Fracture Toughness of Structural Steels", performed at Fritz Engineering Laboratory of Lehigh University under the sponsorship of Bethlehem Steel Corporation. The objectives of the program were (1) to conduct dynamic K_c type fracture tests on two structural steels across a range of plate thicknesses and temperatures, and (2) to explore plasticity concepts in formulating a fracture toughness characterization method in the range of general yielding where the linear elastic approach to fracture toughness evaluation is not possible. This work constitutes essentially the initial efforts of a larger program which was to include four steels and static as well as dynamic K_c evaluations.

It was thought that the dynamic loading rate which provides minimum K_c values would be of more concern to the sponsor than the higher static results. For this reason the static loading experiments were postponed.

The goals of the program were to first use the Lehigh test specimen and drop-weight tear test machine to evaluate K_c values using a linear elastic approach whenever stress conditions permitted. Two plasticity methods were used to obtain "effective" K_c values in the region of general yielding. The initial method, which received most attention, involved measurements of thickness reduction. Exploratory

trial was also given to a method based upon the plastic bend-angle for a specimen with an arrested crack. There was an overlap of data from the dynamic-elastic results and those obtained from the thickness reduction measurements. This overlap region was used to adjust the thickness reduction method. In the region of gross general yielding of the test specimens the plasticity results were the only K_c values available. For this reason additional checks on these methods are desirable.

1. INTRODUCTION

1.1 Definition of K

The simplest method for expressing the measurement of resistance to crack extension employs a parameter, K, termed the stress intensity factor. Using a linear-elastic crack stress field analysis Irwin developed the equations for the stresses near the leading edge of a crack in terms of K and the specimen's physical characteristics.[1] For an opening tensile mode (Mode I) type of fracture of an edge crack in an infinite plate of finite thickness these stresses are represented by the following equations:

$$\sigma_x = \frac{K_I}{\sqrt{2\pi r}} \cos\frac{\theta}{2}\left(1 - \sin\frac{\theta}{2}\sin\frac{3\theta}{2}\right) \quad (1)$$

$$\sigma_y = \frac{K_I}{\sqrt{2\pi r}} \cos\frac{\theta}{2}\left(1 + \sin\frac{\theta}{2}\sin\frac{3\theta}{2}\right) \quad (2)$$

$$\tau_{xy} = \frac{K_I}{\sqrt{2\pi r}} \sin\frac{\theta}{2}\cos\frac{\theta}{2}\cos\frac{3\theta}{2} \quad (3)$$

$$\sigma_z = \mu(\sigma_x + \sigma_y) \quad \text{for plane strain} \quad (4)$$

or

$$\sigma_z = 0 \quad \text{for plane stress} \quad (5)$$

where the coordinates are as shown in Fig. 1. As indicated by the above equations and in the specified figure the analysis of stresses near the leading edge of a crack can be made in terms of the polar

coordinates, r and θ, whose coordinate system originates at the center of the zone of plasticity or non-linear strains located at the leading edge of the crack.

The values of K are usually expressed in units of ksi $\sqrt{in}$ where K is defined as

$$K = \lim \sigma_y \sqrt{2\pi r} \qquad \text{as } r \to 0 \qquad (6)$$

Due to the inconsistency of the existence of a zone of plasticity in a linear-elastic stress analysis, a plastic zone correction is added to the original visible crack length, a_o. It is for this reason, as mentioned above, that the center of the coordinate system used in the linear elastic stress analysis is placed at the center of the plastic zone, at a distance, $a_o + r_Y$, from the edge of the plate and not at a distance, a_o. After introduction of the plastic zone correction, r_Y, the existence of the zone of plasticity is disregarded in the linear elastic solution. The r_Y correction, introduced by Irwin,[2] is given by

$$r_Y = \frac{1}{2\pi} \left(\frac{K}{\sigma_{YS}} \right)^2 \qquad (7)$$

where

$2r_Y$ = diameter of the plastic zone as shown in Fig. 1

K = stress intensity factor

σ_{YS} = yield strength of the material

If the plasticity adjustment factor at the leading edge of the crack is small compared to the thickness of the plate, a plane strain

condition will exist at the crack tip. For the plane strain condition, the value of the stress intensity factor, K, at the point of rapid crack extension or crack instability is termed K_{Ic}, or the "critical" stress intensity factor. This is the lowest possible K factor for the particular material at the testing temperature. If the converse is true and the plastic zone size, r_Y, is not small compared to the plate's thickness, a plane stress condition will exist. This situation occurs due to the lack of elastic constraint through the thickness ($\sigma_z = 0$) and results in various degrees of increase of the fracture toughness, K_c, above the K_{Ic} value.

1.2 Advantages in the Use of K

Cracks in structural components caused in fabrication or developed under service loadings have always been regarded as detractive to the strength of such members. With the advent of the theories of fracture mechanics the engineer is now better equipped to estimate the significance of such cracks on the serviceability and safety of a component.

In the past years, before fracture mechanics became an accepted tool for the engineer, gross assumptions were made in analyzing crack-related structural problems. Sometimes the load was regarded as uniformly distributed across the remaining cross-section neglecting totally the influence of the stress singularity at the crack tip upon the entire stress distribution in the member. Resulting from these analyses were strength estimates which were not realistic.

A common structural problem is the growth of a fatigue crack through the lower flange of the beam up into the web. The crack sometimes forms due to a poor weldment of a cover plate onto the beam's lower flange. Using the theories of fracture mechanics and knowing the crack length and the stress intensity factor, K, for the beam's material, a relatively accurate estimate can be made of the stress distribution in the vicinity of the crack tip, where the stress is critical. This type of analysis can give accurate stress results which would be helpful in estimating the serviceability of the structure and the load at which crack instability will occur.

With the development of higher yield strength steels and their use in bridge design a problem arises in the fabrication of structural components. Larger bridges bring in the use of thicker member sizes which fosters a plane strain condition for fracture in the vicinity of any cracks or flaws. These K_{Ic} type conditions along with the high material yield strength decrease the allowable critical crack size in the component. In order to illustrate this phenomena, look at the following equation for the stress intensity, K, in a finite-width plate with a center crack, $2a_o$

$$K = C\,\sigma\,\sqrt{\pi\,(a_o + r_Y)} \tag{8}$$

where C is a function of the effective crack length, $(a_o + r_Y)$, and the plate width. With K approaching its minimum K_{Ic} value and with σ increasing, with the higher yield strength materials, the effective crack length or flaw sizes resulting from fabrication must be kept to minimum sizes which can be estimated when the fracture toughness is

known. Thus the use of the theories of fracture mechanics are of practical importance.

1.3 Limitations in the Linear Elastic Approach to Fracture Mechanics Due to Specimen Size

Giving attention to the first objective of the project a testing program was devised and initiated in order to calculate the toughness characteristics of the two structural steels across a range of temperature and plate thickness using linear elastic fracture mechanics.

In line with the previous work done at Lehigh University by Madison[3] and Luft,[4] a fixed size test specimen, 3 inches deep and 12 inches long, was employed in the present program. In order for the A441 specimens to satisfy the ASTM K_{Ic} testing requirement[5] relative to specimen thickness and crack size, the calculated K_c value resulting from a drop-weight test would have to be less than 51 ksi $\sqrt{in}$ (using σ_{YS} (dynamic) equal to 80 ksi). When the A441 structural steel was tested dynamically, the resulting K values that were equal to or less than the value designated above usually fell in temperature ranges that were quite low and not of particular interest to the project's goals. At these low temperatures the amount of stable crack growth and plasticity at the crack tip are so small that the results can be applied in a linear elastic fashion using no plasticity adjustment factor, r_Y.

Much attention in the test program was focused on higher temperatures where the resistance to the onset of rapid fracturing is assisted by appreciable amounts of thickness reduction type yielding. Because of this an r_Y correction term for plasticity is added to the initial crack size, a_o, in calculating K_c. This technique theoretically removes the region of plasticity from the analysis and extends the scope of linear elastic fracture mechanics into this region of limited yielding ahead of the crack tip. However, the small amount of stable crack growth that occurs before the onset of rapid fracturing is neglected in this analysis. The resulting moderate effect of this on the K_c evaluations appears to be an acceptable loss in view of the testing simplicity gained by not measuring the stable crack growth. The r_Y correction technique for calculating K_c has its limit at the point of general yielding in the specimen. The K_c value corresponding to this limit is approximately 100 ksi $\sqrt{in}$ for A441 steel. Any characterization of toughness for the steels beyond the region of general yielding warrants another K_c characterization technique, and this is where the second objective of this program comes into focus.

1.4 Plasticity K_c Characterization

Several elastic-plastic theoretical models containing cracks have shown that as the ratio of the net section stress to the yield stress increases towards unity the proportionality between the crack opening displacement, δ, and the square of the r_Y corrected K value tends to remain constant.[6] Direct measurements of the crack opening

stretch were not made, but a correlation was attempted between the thickness reduction and δ where

$$\delta = \frac{K^2}{E\,\sigma_{YS}} \tag{9}$$

It was assumed that δ was proportional to the thickness reduction with a near unity proportionality constant.

Since the majority of the testing was done in the drop weight machine all measurements of thickness reduction had to be made after the fracture had occurred. Except for measurements of maximum load, "in-test" measurements were considered to be beyond the scope of the program.

A preliminary study was made of the thickness reduction contours ahead of the fatigue crack in a fractured specimen. A sample result is shown in Fig. 2. This figure shows how the thickness reduction contours expand just ahead of the fatigue crack and reach limiting or constant positions some distance ahead of the crack. Comparing this contour profile to a typical R-resistance curve,[7] shown in Fig. 3, it was reasoned that the initial expanding contours were related to the rising portion of the R-curve where the plastic zone develops with some small stable crack growth. In this region as the material's toughness increases and as the driving K reaches the critical K, unstable crack motion starts and continues at the plateau value. The plateau value of K_R (termed K_M) on the R-curve was reasoned to correspond to the region of constant thickness reduction.

A method relating this plateau K value to the thickness reduction was devised, and it furnished a measuring technique to calculate K_M under conditions of gross general yielding. Concern over the amount of stable crack growth that occurs before the onset of crack instability (which might now be significant in the region of general yielding) is unwarranted because the devised technique is applied beyond the stable crack growth region. The method involves equating the thickness reduction to δ at a formulated normal distance from the flat tensile portion of the fractured surface. This technique was employed at set distances forward from the fatigue crack. Two such distances or sections were used to calculate K_M or an "effective" K_c because it seemed desirable to use more than one measurement for averaging purposes.

In the dynamic tear-tests of the higher yield strength structural steels another K_c measuring technique was planned and received exploratory trial. Due to the high degree of toughness of these steels near room temperature, the test specimens sometimes failed to fracture completely after the release of the drop-weight. What usually did result was a noticeable amount of crack movement down into the specimen with the development of a plastic hinge whose bend-angle was easily measured. Assuming that this plastic hinge possessed an axis of rotation at the center of this ligament, a value of the crack opening stretch, δ, was calculated by means of simple geometry knowing the bend-angle, β, the size of the net ligament, and the location of the elastic-plastic boundary. Due to the uncertainity of

the location of this boundary in a Mode I displacement condition, an arbitrary constant, λ, was included in the solution. Its value was determined experimentally. When the value of δ was determined an effective K_c value was calculated using Eq. (9).

1.5 Minimum K_c Levels

The steels being tested were loading-rate sensitive (common) structural steels. As a result measurements of minimum K_c levels were considered most important. Using the graph shown in Fig. 4 it was felt that using a loading time of 0.5 to 1.5 milliseconds ($1/t \approx 1 \times 10^3$ sec^{-1}) would result in minimum K_c levels. This loading time was used in the drop-weight tear tests and its use was supported by the fact that in many of the dynamically tested specimens, crack arrest patterns were visible on the fractured surface. This proved that the cracking velocities were at a minimum and that K was near the value corresponding to crack arrest. From Fig. 4 the calculated K_c values can be regarded as minimum values.

2. DESCRIPTION OF TESTS

2.1 Specimen Size and Material

The test specimens used in the drop-weight tear tests were 12 in. long by 3 in. deep as shown in Fig. 5. The thickness of the specimens tested were 1/2", 1", and 2" and the materials principally tested were A441 and RQ100-B structural steels. The chemical and physical properties of these two steels are shown in Table 1. The RQ100-B structural steel is a Bethlehem Steel product which was given a special heat treatment for this program to provide a yield strength of about 80 ksi, rather than 110 ksi, as would be normal for the commercial product.

2.2 Specimen Preparation

All the specimens were saw-cut from the original 6 ft. by 4 ft. plate similar to the pattern shown in Fig. 5. In the saw-cutting process any heat-affected regions were removed from the test specimens.

All of the specimens were saw-cut with their long dimension in the rolling direction. This resulted in a crack toughness characterization pertaining to crack motion perpendicular to the rolling direction of the steel. This direction was studied because the resistance of the steel to crack propagation in this direction is higher and more uniform than for crack motion parallel to the rolling direction. Besides, in

structural applications the rolling direction is usually made to correspond to the direction of largest tension.

After the individual test specimens were saw-cut from the plates the top and bottom surfaces of the specimens were shaped to assure parallel surfaces. This was done to assure specimen stability during the fatigue cracking process. The sides of the specimen were surface ground to assure a uniform thickness throughout an individual specimen. This was required for the thickness reduction technique of evaluating K_c. The tolerance in the thickness direction was $\pm$ 0.001 in. A 90° Chevron notch was machined in the center of the specimen as shown in Fig. 6. The recommended angles of taper, α, for the notch are 45°, 45°, and 29° respectively for the 1/2", 1", and 2" thicknesses. The Chevron notch was used to help initiate crack growth in the fatigue process.

The fatigue crack growth was done on a 10-ton Amsler Vibrophore, which is a high frequency fatigue testing machine. The test specimens were placed into the machine in a three-point bend arrangement, and the fatigue cracking was done in two stages, a fast and a slow growth portion. During the fast growth stage, the crack was driven down into the specimen to the depth, a_F. The main purpose of this fast growth portion was to get the crack well into the specimen in a short period of time. Accordingly, no fatigue cracking criteria was followed during this particular portion of crack growth. As mentioned above, the only requirement adhered to was to get the fatigue cracking done quickly. Approximately 20 minutes was considered acceptable.

The criteria followed in the slow growth portion of the fatigue cracking process was that the average crack growth rate over the slow growth distance, a_s, be equal to or less than 1 microinch per cycle.[5] Shown in Fig. 7 is the data used in fatigue cracking the A441 steel. Of importance in this data are the final K levels at the crack tip at the end of the slow crack growth portion.

According to ASTM K_{Ic} testing specifications[5] on fatigue crack pre-cracking, the final K level at the end of the fatigue crack should be equal to or less than one-half of the expected K_c value resulting from a fracture toughness test. However, there is still some disagreement as to the necessity of the ASTM fatigue pre-cracking requirement. Furthermore, our method of pre-cracking (1 microinch per cycle) was above the ASTM rule only for the low testing temperatures which were of secondary interest to the project.

In many instances during the fatigue cracking process the crack in the test specimen tended to grow faster on one side than on the other. In order to straighten out the crack leading edge a steel wedge was forced into the machine notch on the side of the specimen where the crack was longer. This prevented the longer side of the crack from cycling through the complete stress range, thereby slowing its growth rate, while allowing the other and shorter crack to continue to grow. When the edges of the crack reached equal length on both sides of the specimen the wedge was removed and the regular fatigue cracking process was continued.

2.3 Test Apparatus - Dynamic K_c Tests

The dynamic fracture tests were done in a drop-weight tear test machine, shown in Fig. 8. The main uprights of the machine are two W12X85 columns to which are bolted fabricated tee-sections along which the drop-weight rides. The bolts allow for realignment of the rail system. The drop-weight machine has a drop-height capacity of approximately 20 feet. There are side grooves in the drop-weight which cause it to ride along the web of the tee-section. A close tolerance of 1/16 in. exists between the falling weight and the rail system so that upon release there is negligible "wobbling" or locking of the weight along the rails.

The weight of the falling mass is 400 pounds. The original weight, 200 pounds, was doubled in size in order that lower drop-heights could be used in the dynamic tests to impart the same amount of energy to the test specimens as would a smaller weight falling from a greater height. This was done to help lessen the influence of the test specimen's inertia on the load record. The additional weight also doubled the energy capacity of the drop-weight machine. The original weight was increased by bolting onto it two plates weighing approximately 100 pounds each. These plates were set on opposite sides of the original weight.

The drop-weight is raised and lowered to the required drop-heights by means of a 2-ton overhead crane. Once the weight has been positioned at the required elevation above the test specimen it is released by an electomagnetic release mechanism. After the weight

fractures the specimen, the falling weight is stopped by two shock absorbing supports made primarily from neoprene rubber.

At the bottom of the drop-weight is the tup which serves also as the load dynamometer. The tup is positioned snugly in a recess at the bottom of the weight and is fastened into place by a long bolt passing vertically through the weight to its top. The tup is the load measuring part of the test apparatus, and it is shown in Fig. 9. The load dynamometer is machined from 4340 maraging steel and it is heat treated to Rc 50. Two four-arm bridges are instrumented onto the tup with a 500 ohm strain gage passing across each arm of the bridge. The resistance of the gages were increased from 240 ohms in order to give the load signal greater sensitivity. Two bridges were placed on the tup as a precautionary measure in case one bridge failed in operation by shearing off due to the repeated shock loadings. A four-arm bridge is used to measure the axial load in the dynamometer, and by its very use any bending that might occur in the tup upon impact with the test specimen is removed from the load signal.

As an aid in decreasing the influence of the specimen's inertia on the load record, 3/4 in. long, 1/2 in. diameter half-rounds were used during each drop-weight fracture test. The positon of the pad relative to the test specimen is shown in Fig. 10. When the tup makes contact with the half-round, a considerable amount of deformation occurs in the pad with a corresponding large amount of energy absorption. This cushions the application of the load onto the test specimen and,

as a result, stretches out the loading time. The half-round cushions were machined from drill rod.

The loading dynamometer has a 147^{o} included angle ground into its tip. The original shape of the tup's tip was a semi-circular. The mild-angled tip was used in this program as to reduce the cushion's resistance to initial deformation.

The load signal is recorded on a Tektronix Type 549 storage oscilloscope with a "Type-Q Transducer and Strain Gage Preamp Plug-In Unit" used to monitor the signal. This particular oscilloscope is equipped with a delay mechanism whereby the start of the trace can be delayed for a specific time interval and then started and stored on the oscilloscope screen. It was because of these requred features that this oscilloscope was obtained by Madison[3] and Luft[4] for use in the drop-weight tear tests.

A photocell is attached to the drop weight machine, as shown in Fig. 8, and when the weight is released and starts its free fall, a shutter attached to the drop-weight breaks the light beam of the photocell and sends a triggering signal to the oscilloscope to initiate the sweep of the trace. Depending on the drop-height of the particular test, a corresponding particular delay time is set on the oscilloscope's delay mechanism. When the triggering signal is monitored by the oscilloscope the delay mechanism is activated, and when the set delay time passes, the load signal from the four-arm bridge of the tup is recorded and stored on the oscilloscope. The intention of the delay mechanism is to set as the delay time the time

required for the drop weight to pass the photocell and make contact with the test specimen. In this way the trace recorded on the oscilloscope will show a record of the load in the tup beginning with first contact against the test specimen. These delay times vary depending on the initial height of the drop-weight before release. These times were initially measured by a method of trial whereby the weight was dropped onto a solid bar from a definite prescribed height and the delay times were varied until the load signal was properly recorded on the oscilloscope. A Polaroid camera is used to take a picture of the load signal stored on the oscilloscope screen in order to have a permanent record of each fracture test.

On the surface of the test specimens opposite the Chevron notch a 1/16 in. diameter hole was drilled 3/4 in. deep into the specimen at the center-thickness, offset 1 inch on either side of the plane of the notch. Into this hole was placed a chromel-alumel thermocouple which provided for the recording of the specimen temperature before each test. The specimens were heated in an oven or cooled in a household refrigerator, in a deep freeze, or by means of dry ice depending on the required test temperature.

2.4 Test Apparatus - Thickness Reduction Type K_c Tests

In the thickness reduction technique a Gaertner Series M1180 traveling microscope was used to measure the thickness reductions on slices cut from the fractured specimens. The microscope has a range of 2 in. and can read directly down to 0.0001 in. Since thickness

(or thickness reduction) measurements were required at different normal separations from the brittle or flat portion of the fracture surface, calibrated movement perpendicular to the fracture surface, or in other words, movement perpendicular to that furnished by the microscope travel was required. To furnish this the shimming assemblage shown in Fig. 11 was machined, assembled, and mounted to the base of the microscope. This setup allowed for movement in 0.005 in. increments away from the fracture surface and perpendicular to the thickness direction.

To aid in these thickness reduction measurements slices were saw-cut from the fractured specimen. These slices furnished two surfaces whose edges corresponded to the thickness or thickness reduction profile at specific locations away from the end of the fatigue crack. These slices conveniently fitted into the shimming assemblage, as shown in Fig. 11, for thickness measurements.

2.5 Test Procedure for Dynamic K_c

On the day previous to testing, the specimens to be tested were placed in the required test-temperature atmosphere and were allowed to stay in this temperature for 12 hours or more. This assured uniform temperature distribution in each specimen. At this same time the thermocouple was placed into one of the specimens to be tested so that the temperature levels could be monitored.

On the day of testing the oscilloscope was switched on first so that it had ample time to heat. The load signal originating from the four-arm bridge on the load dynamometer was zeroed in on the oscilloscope screen and calibrated. During this process the drop-weight was suspended, assuring no load in the tup. The photocell was checked by passing an object through the light beam to see if it was triggering properly. The electromagnetic release mechanism's circuit was also switched on and checked. With the safety pin inserted in the release mechanism, the release button was pressed to check if the system was operating correctly. The safety pin prevented the release of the drop-weight once it had been raised from its resting position on the shock absorbing supports. Just before the actual fracture test the safety pin was removed.

Knowing the testing conditions - temperature, specimen size and yield strength - the general results of the particular test were estimated based on the experience acquired from previous tear-tests. Having some idea of the general outcome of the test a sufficient drop-height was selected. The height was kept near the minimum necessary to induce fracture upon impact of the drop-weight onto the test specimen. This practice also tended to reduce the test specimen's inertial effect on the load record. After the drop-height was selected a corresponding delay time was set on the oscilloscope. Also, having some general idea of the expected fracture load, the magnitude of the intervals on the ordinate axis of the oscilloscope screen was set.

After all systems were checked and found to be functioning properly, a final temperature reading was taken of the test specimen.

The temperature was recorded, and the specimen was immediately placed onto the test fixture of the drop-weight machine. The specimen was aligned so that the load dynamometer would hit the specimen directly over the fatigue crack. Then the required number of half-round cushions were placed on the specimen. The number of cushions varied depending on the expected magnitude of the fracture load. The safety pin was now removed from the release mechanism, and the drop-weight was raised to its required height. After reaching this height the drop-weight was released immediately and the test specimen was fractured. Except in the case of occasional maladjustments of the electronic equipment, a load-time signal was recorded and stored on the oscilloscope screen. A Polaroid photograph was taken of the trace.

The two halves of the fractured specimen were removed from the drop-weight machine and brought to room temperature. After the fracture surfaces were cleaned and dried by use of a compressive air jet, a thin coat of a clear acrylic lacquer was sprayed onto the surfaces to act as a protective coating.

Since each dynamic fracture test required approximately one minute to complete once the specimen was taken from its test-temperature atmosphere, no facilities were used to keep the specimen in its test-temperature atmosphere while seated on the dynamic test fixture. Any temperature gradient within the test specimen was assumed negligible.

Knowing the test temperature and the loading time for each test specimen, their effects on the yield strength of each specimen

considered, and a dynamic yield strength was calculated. By means of an equation for K, developed by Gross and Srawley for three-point bend specimens and revised by Madison[3] and Luft[4] for the Lehigh specimen, a K_c value was estimated using the maximum recorded load as the fracture load.

2.6 Test Procedure for Thickness Reduction Type K_c

A number of the dynamically tested specimens were measured for thickness reduction. One-half of the fractured specimen was selected and a slice was taken from it as shown in Fig. 12. The saw-cuts were made so that the slice represented the measurement positions, B/2 and 3B/4, away from the end of the fatigue crack. These slices were also wet ground to remove the rough edges resulting from sawing. The edges of each slice were also gently finished with a fine emery cloth to remove burrs resulting from the grinding. This resulted in true thickness contours at the measurement positions. The slice was now ready for thickness reduction measurements.

Before any measurements could be taken the microscope was first aligned as perfectly as possible with the shimming assemblage which was mounted to the base of the microscope. This meant that the microscope travelled parallel to the edges of the assemblage and perpendicular to its sides. The slice was then placed on the sliding measuring platform and clamped in position, as shown in Fig. 11. With the turn-screw in its loosened position the sliding platform was manually pushed back and forth, while the edge of the slice was aligned with the

y-direction crosshair of the microscope. This guaranteed that the slice was positioned parallel to the four sides of the shimming setup.

The turnscrew was tightened with no shims. The microscope was then moved until its x-direction crosshair was aligned parallel to a "weighted" fracture surface or zero position. The word, "weighted", is used because the unevenness of the actual fracture surface required judgment in the selection of an average position. This movement of the microscope in aligning the x-direction crosshair does not hamper the other fixed alignments. The steps in the alignment of the microscope and slice are illustrated in Fig. 13.

The first estimate of r_Y and, in turn, K_c from thickness reduction pertained to a depth of B/9 from the fracture surface. Being unable to measure exactly at this distance away from the fracture surface, measurements of thickness were made at distances slightly larger and smaller than the value of B/9. The thickness at the gage position B/9 was linearly interpolated between the two measured distances. Assuming the measured thickness reduction equal to the crack opening stretch, δ, the corresponding plastic zone size, r_Y, was calculated and the ratio of r_Y/B was evaluated. A new measuring position away from the fracture surface was now calculated knowing the ratio of r_Y/B from the previous measuring position. At this new position the thickness was again measured; a thickness reduction was found; r_Y was re-evaluated using δ equal to this new thickness reduction; and a new ratio of r_Y/B was again calculated. Using this newly calculated value of r_Y/B another measuring position was found. This process was repeated until there was a convergence of the previous and newly calculated positions in a

particular step. When this occurred the δ value pertaining to this "equilibrium" position was used to find the "effective" K_c value. An example of the measuring procedure is given in Appendix 1.

The measuring procedure is made easier once the first position, B/9, and the second measuring position are known. These positions correspond to the values of S_n in line 1 and 2 of Appendix 1. These two positions are the maximum and minimum distances at which thickness reduction measurements will be required. Since the equilibrium position will have to lie somewhere between them, a group of thickness reduction measurements are first made covering this entire range. This is done using the 0.005 in. thick shims, and this is shown in the top half of the sample calculation of Appendix 1. This allows the converging process to be handled quite easily, and this is shown in the bottom half of Appendix 1.

Now that the test procedure has been described, a few additional words are needed concerning the previously described slicing procedure. In this procedure it was explained how a slice was removed from one-half of the fractured specimen. Care should be taken in selecting the proper half to use for the slice. That half of the specimen should be used which retained both shear lips upon fracture. The typical slice in Fig. 12 is an example of such a selection. This type of slice permits the measurement of the thickness below the fracture surface because of the physical presence of the shear lips.

If the shear lips are shared between both halves, personal judgment should be used in selecting which half of the specimen to slice. If this situation is so pronounced that thickness measurements are not possible across the slice because of the absence of material at one edge of the slice, a different measuring procedure is required. This missing material corresponds to the shear lip existing on the other half of the fracture specimen. For this situation the measuring procedure is exactly the same except that the slice is shimmed so that measurements can be made at equal distances above and below the fracture surface or zero position. In other words thickness measurements are taken above and below the fracture surface at equal distances, and the measurements are made from the centerline of the slice out to the edge of the slice where the shear lip exists. The total thickness for a particular distance away from the fracture surface is, therefore, taken to be the sum of the two half-thickness measurements made above and below the fracture surface at the same distance. The centerline of the slice must be physically scribed onto the slice for this method. The remaining measurement steps are the same.

2.7 Test Procedure for Bend-Angle Type K_c

In several of the drop-weight tear tests the test specimen failed to fracture completely due to its high degree of toughness at near room temperatures. The drop-weight was usually at its maximum safe operating drop-height for such a test. This maximum safe height was decided to be

10 feet, and a greater height was not used in fear of damaging the load dynamometer or the strain gages instrumented onto it.

After such a test the partially fractured specimen was removed from the drop-weight machine, and the bend angle, β, was measured by means of a protractor. The specimen was then placed into the deep freeze or in contact with dry ice. After being in this cold atmosphere for several hours it was again placed into the drop-weight machine where the fracture of the specimen was completed. No data was required during this second drop. Its purpose was just to complete the break of the specimen. As before the broken specimen was warmed to room temperature, dried, and the fracture surface sprayed with the protective lacquer coating.

Inspection of the fracture surface of the broken specimen clearly distinguished to what depth the crack moved during the first drop of the weight at the warmer temperature. The remaining ligament cross-section was more brittle in texture compared to the ductile failure plane of the initial drop. This difference in appearance easily led to the location of the final crack arrest position resulting from the first drop and accordingly showed the cross-section of the previously unbroken ligament. Since the final crack arrest position was never perfectly straight, a "weighted" straight position was selected along the actual arrest edge. Having determined the dimensions of this "weighted" cross section, its depth was halved, and this position was assumed to be the axis of rotation of the plastic hinge. Now knowing this position and the bend-angle resulting after the first

drop of the weight, the crack opening stretch, δ, value was calculated using simple geometry, Fig. 14, according to the following equation

$$\delta = \left(\frac{L_{Lig}}{2} + \lambda \frac{n}{n+1} \frac{\delta E}{4 \sigma_{YS}} \right) \beta \qquad (10)$$

where β is in radians. The second term in the parentheses was included as an adjustment in locating the elastic-plastic interface, the location for the δ definition. The "effective" K_c value was calculated using Eq. (9).

3. THEORETICAL ANALYSIS

3.1 Experimental Analysis for Dynamic K_c

Using a boundary collocation technique Gross and Srawley developed an expression for K for single-edge-cracked plate specimens in three-point bending.[8] This expression for K is represented by a fourth degree polynomial of the following form, with values of the coefficients A_W furnished for values of a/W up to 0.6:

$$Y = \frac{K\ B\ W^2}{1.5\ PL\ \sqrt{a}} + A_o + A_1 \left(\frac{a}{W}\right) + A_2 \left(\frac{a}{W}\right)^2 + A_3 \left(\frac{a}{W}\right)^3 + A_4 \left(\frac{a}{W}\right)^4 \tag{11}$$

where

Y = dimensionless ratio

B = specimen width

W = specimen depth

P = applied load

L = span length

a = effective crack length

A = coefficients whose values are dependent on the specimen's L/W ratio

The coefficients for the above equation have been developed for L/W ratios of 8 and 4 and are shown in Fig. 15.

Since the same three-point bend configuration was used in the dynamic fracture tests, the above K calibration was employed for the solution of the dynamic K_c values. However, due to a specimen length-to-width ratio of 3.33 which was the L/W ratio used in this program, a different set of coefficients, other than those developed by Gross and Srawley, had to be derived for use in Eq. (11).

This new set of coefficients was obtained[4] by simply linearly extending those values of A_w recommended by Gross and Srawley to the L/W value of 3.33. The results of this extension are presented also in Fig. 15. As a check, a compliance calibration was made for the bend specimen whose L/W ratio was 3.33 and it was shown that the above linear extension of the Gross-Srawley data was valid.[4]

3.2 Mathematical Solutions for Dynamic K_c

Using the equation for the plastic zone size, r_Y, Eq. (7), in an adjusted form

$$K = \sigma_{YS} \sqrt{2\pi\, r_Y} \tag{12}$$

and substituting this expression into Eq. (11) results in

$$\frac{r_Y}{W} = \frac{P^2 L^2}{B^2 \sigma_{YS}^2 W^4} \frac{2.25}{2\pi} \frac{a}{W} Y^2 \tag{13}$$

Letting

$$F = \frac{2.25}{2\pi} \frac{a}{W} Y^2 \tag{14}$$

Eq. (13) can be rewritten

$$\frac{r_Y}{W} = \frac{P^2 L^2}{B^2 \sigma_{YS}^2 W^4} F \qquad (15)$$

Next dividing both sides of Eq. (15) by an arbitrary constant, Q, results in

$$\frac{\frac{r_Y}{W}}{\frac{QP^2 L^2}{B^2 \sigma_{YS}^2 W^4}} = \frac{F}{Q} \qquad (16)$$

Using Eq. (16) Fig. 16 illustrates the graphical technique that may be employed to solve for K or K_c. Figure 16 is a plot of Eq. (14) with F versus (a/W). The technique involves the solution of two similar triangles. Once the value of (r_Y/W) is scaled off the graph and r_Y is known, a value of K can be evaluated using Eq. (12). The value of K becomes K_c when the applied load, P, used in the solution is the fracture or maximum load recorded during the drop-weight tear test.

Due to the length of time required in such a graphical solution when many specimens are involved, a computer program was developed to solve for the values of K_c. A simplified flow chart of the computer program is shown in Fig. 17. Essentially the method of solution involves an iterative process where a value of (r_Y/W) is assumed, and this value is used, in turn, to calculate another (r_Y/W) value by means of Eq. (13) remembering that

$$\frac{a}{W} = \frac{a_o}{W} + \left(\frac{r_Y}{W}\right)_{\text{assumed}}$$

When the difference between the assumed and calculated values of (r_Y/W) is equal to or less than 0.0001 inches the iterative process is stopped and a K value evaluated using Eq. (12). The computer solution was the method used in all the K_c computations.

Table 2 lists the K_c values that resulted from the dynamic drop-weight tear tests on the A441 and RQ-100B structural steels. Graphs of K_c versus temperature for both the structural steels are shown in Figs. 18 to 22.

3.3 Dynamic Yield Strength

In the previously discussed solutions for the dynamic K_c values, the value of the yield strength, σ_{YS}, appeared in several of the equations. As a result a knowledge of the change in the yield strengths of the materials tested with differing test conditions had to be acquired.

In the drop-weight tear tests the rate of load application onto the test specimens was very high resulting in very high strain rates in the material. Also the test temperatures of the specimens varied from a high of approximately $+150^{\circ}$ F to a low of about -80° F. Both the high strain rates and the changing test temperatures have an effect on the yield strength of each particular test specimen.

A test program investigating the dynamic yield conditions of the different materials could have been undertaken, but this was considered simply outside the capacity of the program. Instead the following empirical expression was used:

$$(\sigma_{YS}) = (\sigma_{YS})\Big|_{+75^{o}\ F, t_o} + \frac{174{,}000\ \text{ksi}}{\log(2 \times 10^{10} f)(T + 459)} - 27.4\ \text{ksi} \qquad (17)$$

where

t = loading time to maximum load

t_o = time of load application for a static test (50 sec.)

T = testing temperature in ^{o}F

This expression was suggested by Irwin[9] as a best fit for data on A302B Steel from Ripling and for data on 3-Ni-Cr forging steels for Wessle. It takes into account both the strain rate and the material temperature on the yield strength. This equation is considered to furnish best fit conditions for any structural steel whose static yield strength is not greater than approximately 120 ksi. Madison[3] and Luft[4] showed that A441 steel behavior agreed approximately with this equation.

3.4 Investigations into a Typical Load Record Response

Figure 23 shows a sketch of a typical load record. This is a depiction of the load signal as it is recorded and stored on the oscilloscope after each successful fracture test.

The sketch includes two different types of load response, one represented by the solid curve and the other by the dashed curve. The solid line depicts a load record resulting when the half-round steel cushions are used during the fracture test. These cushions stretched out the loading time, from zero to maximum load, to approximately 0.5 to 1.5 milliseconds. These loading times resulted in values for the inverse of loading time (1/t) which guaranteed load responses that would lead to minimum K_c levels (Fig. 4). During this loading period a

change in slope was witnessed in the load record. It is believed that during the initial period of loading or when the slope of the curve is less severe, deformation of the cushion was progressive with an increase in load. At the change in slope, the pad material had strain hardened enough to prevent further deformation. The maximum recorded load was taken as the fracture load, P_c, which was used in all the K_c calculations. After reaching maximum load, the load record fell off either sharply or gradually, depending on the severity of the type of fracture.

In a majority of the load records, oscillations were found to exist that were periodic in nature, as shown in Fig. 23, and so a study was made into the possible sources of vibration in the test setup during a drop-weight tear test. The oscillations were observed after the maximum load and while a load was still being applied to the test specimen. It was felt that vibrations were interacting with the actual fracture process because the drop-weight was actually fracturing the specimen during this time period. The results of the study of expected vibration time periods is shown in Fig. 24.

First investigated was the reflected wave motion in the drop-weight caused by its initial sudden contact with the test specimen. This wave motion corresponds to the travel of a compression wave up from the tup to the top of the weight where it is reflected back down to the tup as a tensile wave. The period for one such complete cycle was calculated to be 2.3×10^{-4} sec.

Investigated next was the bending response of the test specimen. In these calculations the specimen was considered to be a spring with the 400 lb. weight vibrating above it. The spring constant for the specimen was calculated taking into consideration the crack in the specimen. The period for this response was found to be 8.4×10^{-3} sec. These vibrations never could appear on the trace because within this relatively long time period the fracture of the test specimen occurs almost immediately, destroying the integrity of the specimen and the source of any vibrations.

The last type of vibration investigated was the shear wave motion in the test specimen. This study is directly analagous to the reflected wave motion in the drop-weight, described previously, except that in this instance the path of travel of the reflected wave is from the center of the test specimen, where the tup strikes, to either of the specimen's supports and back to the center. The wave motion involved is a shear wave motion and can be regarded as a high frequency contribution to bending of the specimen. The period for this complete cycle was calculated to be 0.8×10^{-4} sec.

Measuring the period of the oscillations visible in the load records resulted in a period whose value was approximately 4.0×10^{-4} sec. This value is in reasonable agreement with the calculated value of the period for the reflected wave response. In fact it is felt that these oscillations do originate from these reflected waves, and that the difference that does exist between the calculated and measured values of the periods is believed to be caused by some dampening originating in the two additional plates that were bolted onto the

drop-weight. These are the plates that were attached to the original weight in order to increase its weight up to 400 lbs. No other vibrations of significant size could be found on the test records.

If the half-round steel cushions are not used during a fracture test, the resulting load record is depicted by the dashed curve in Fig. 23. The shape of the rising portion of the curve is similar to that when a pad is used. Some cushioning resulted from the indentation of the tup into the test specimen. The change in slope may be caused by the strain hardening of the deforming material under the tup. The loading time for this type of load record corresponds nearly to the shear wave period and represents the main inertial response of the test specimen to the rapidly applied load. This load record cannot be regarded as valid because it is elevated by the inertia of the test specimen. Studies by Madison[3] and Luft[4] indicated that the second load maximum was in approximate agreement with the bending moment in the specimen, measured directly by strain gages on the specimen. However, in the tests reported here this "second maximum" technique was not employed.

3.5 Experimental Analysis for the Thickness Reduction Type K_c

In an attempt to formulate a plasticity oriented fracture toughness characterization procedure, several of the elastic-plastic theoretical models having an elastic-plastic behavior in the presence of a crack have been investigated. It was found that as the ratio of the net section stress to yield stress increased towards unity a

constant proportionality was maintained between the square of the r_Y corrected K value and the crack opening stretch, δ, Fig. 1. This suggested that in the region of general yielding the plastic strains in the vicinity of the leading edge of the crack remained proportional to K^2.

Direct measurements of crack opening stretch were not attempted in the dynamic fracture tests because of the instrumentation difficulties involved in such a task. However, success has been registered by laboratories in correlating the crack opening stretch to the thickness reduction adjacent to the crack tip when the thickness reduction was greater than one mil. These results showed that a proportionality existed between the δ values and the thickness reduction measurements when these measurements were made at the deepest point of thickness contraction at the crack tip. The constant of proportionality was nearly unity.

In the dynamic fracture tests it was reasoned that the K values driving the crack initially increased until the critical K was attained with the increase in load up to P_c. At this critical value unstable crack growth began, and the K level continued to increase with increased fracture surface roughening until the limiting plateau value, K_M, was attained. This reasoning is consistent with the R-curve concept as discussed earlier.

These considerations were supported by a thickness reduction study made on several of the test specimens after fracture. This study

resulted in thickness reduction contours ahead of the fatigue crack which corresponded to the above R-curve reasoning. The initial contours developed rapidly ahead of the fatigue crack position attesting to the sharp increase of material toughness and its unwillinghess to fracture. This region of sharp contour development is analagous to the rising portion of the R-curve where the plastic zone develops with some small stable crack growth. As the contours further developed they gradually levelled off to constant positions, and this was where it was felt that the crack was moving at the plateau, K_M, level, similar to the shelf or plateau of the R-curve. These considerations suggested that the magnitude of the thickness reduction some distance ahead of the initial crack tip where the contours are uniform may serve usefully as a measure of the plateau value of K on the resistance curve or of an "effective" K_c value.

3.6 Empirical Solutions for Thickness Reduction Type K_c

Based on the physical reasoning several empirical thickness reduction measurement techniques were attempted in order to formulate a fracture toughness characterization in the area of general yielding. A slice was removed from either half of the fractured specimen so that its surfaces were perpendicular to the brittle portion of the fractured surface and so that these same surfaces corresponded to distances, B/2 and 3B/4, ahead of the final fatigue crack position. These distances were selected so that measurements of thickness reduction made along these surfaces would correspond to a region along the test specimen

where the thickness reduction contours were in the leveled off position. Two positions seemed desirable to employ for the measurements for averaging purposes.

A surface further away from the fatigue crack and a larger separation between surfaces would have been preferred so as to insure measurements of thickness reduction in the region of uniform contours, and, in turn, constant K levels. However, there were two physical limitations prohibiting these choices. First of all the load usually tended to expand the specimen where it made compressive contact so that the thickness reduction measurements in this region had to be avoided. Secondly the positions selected had to accommodate all the plate-thicknesses tested. In regards to these points, the validity of the 3B/4 position in the 2" specimens was destroyed by the bulging of the material caused by the tup, and so only one surface was used for the K_c computations.

The first technique attempted called for measuring the thickness reduction at distances away from the brittle portion of the fracture surface and evaluating the respective r_y values for these positions. Using the hypothesis that the thickness reduction equaled the crack opening stretch the position was found which equalled one-half of r_y calculated for that particular position. This position was selected as the balanced point in the measuring procedure, and the r_y values corresponding to this location was used to evaluate the K_c value for the specimen. This procedure, however, failed to function properly for all the plate thicknesses of A441 steel, and accordingly it was abandoned.

The second attempt called for equating the thickness reduction to the crack opening stretch at a distance, S, away from the brittle or flat portion of the fracture surface where S, the new balanced position, is given by

$$S = \frac{1}{3} B f \left(\frac{r_Y}{B}\right) \tag{18}$$

where

$$f \left(\frac{r_Y}{B}\right) = \frac{(r_Y/B)^{1/3}}{1 + 2(r_Y/B)^{1/2}} \tag{19}$$

The above function of r_Y and B reaches a maximum value of one-third when r_Y equals B. For any values of r_Y/B greater than 1, Eq. (19) was ignored, and the term, $f(r_Y/B)$, was assumed to remain constant at a value of one-third. This second technique and the values resulting from its use are depicted in Figs. 18 to 22. This is also the technique used in the sample calculation of Appendix 1.

Briefly referring to the K_c values obtained from the thickness reduction technique, a plot of these K_c values versus temperature should be displaced somewhat above the curve obtained from the dynamic K_c values in the region where the two methods overlap because the thickness reduction K_c values refer to the plateau value on the resistance curve as opposed to the smaller but true K_c values corresponding to the points of tangency of the G and R curves in the dynamic K_c values. The point of tangency represents the point of crack instability and the start of the rapid fracture process.

3.7 Experimental Analysis for the Bend-Angle Type K_c

As a second attempt in formulating a plasticity based fracture toughness characterization a bend-angle type of K_c measurement procedure was explored. As in the thickness reduction technique it was reasoned that in the dynamic fracture tests the K value driving the crack increased until the critical K level was attained whereupon unstable crack propagation began. Again the K level increased to the plateau value with increased fracture surface roughening. However, due to a lack of available energy caused by an insufficient drop height the fracture process ceased and the crack arrested. Resulting was a partically fractured specimen with a measurable bend-angle, β.

Using these considerations it was felt that the K level corresponding to the crack arrest would represent the plateau value since it was at this value that the crack was propagating when it arrested. Accordingly it was reasoned that the K value resulting from any bend-angle type computation would be a plateau value.

The bend-angle technique consisted in measuring the bend-angle after the initial partial fracture; completing the fracture of the specimen at a very cold temperature; measuring the depth of the net ligament resulting from the first drop and calculating the crack opening stretch, δ, using simple geometry. The specimen was assumed to rotate about a plastic hinge whose center of rotation was at the middle of this net ligament. The δ value was calculated at the elastic-plastic interface, where δ is defined, and for this reason a correction term had to be included in the calculations. This correction was

taken from Mode III (shear) displacement theory, and for this reason there is uncertainty in how it should be applied to the Mode I (tensile or opening) displacement condition. To allow for this uncertainty an arbitrary constant, λ, is introduced. Its value will need to be determined by calibration experiments, but preliminary results indicate that it should be between 0 and 1 in order to produce reasonable results, as one would a priori expect. The initial results of the bend-angle technique are presented in Fig. 25 for A514 2" plate.

In such a procedure it was hoped that the crack propagated through at least one-half of the original cross section. This assured that the arrested K value was on the plateau of the R-curve. A smaller crack movement could not assure this, while too large a movement might result in excess plastic deformation of the small net ligament after crack arrest, tending to produce larger β values than wished for.

4. RESULTS AND DISCUSSION

One portion of the program consisted in investigating and improving the drop-weight tear test procedure. A vibrational study was performed in order to find the origin of periodic oscillations appearing on most of the load records. This study concluded that these oscillations were caused by the reflected compressive-tensile wave motion traveling up and down the drop-weight after its initial sudden contact with the test specimen. The corresponding vibration period is small compared to the loading time and these vibrations appear to have no significant affect on the maximum load used for K_c computations.

Several different cushioning methods intended to remove the "inertial" spike at the start of the load record were investigated. First of all increasing the weight of the drop-weight (to reduce the impact velocity) and adding a large-angle wedge shape to the striking region of the tup was ineffective toward removal of specimen inertia. This is understandable because the velocity decrease was moderate and the large included angle of the wedge permitted a very rapid increase of the loading force. The best results were found to occur when the half-round cushions of unhardened tool steel were used. These withstood the dynamic loading conditions satisfactorily and caused a sufficient decrease of loading rate so as to remove the inertial spike. As a result of all modifications the loading times for this

program were increased nearly by a factor of two over the typical loading times for the Madison[3]-Luft[4] testing program.

The graphs of Figs. 18 to 22 show the results from the present program in comparison to the Madison-Luft results. The immediate conclusion drawn from the results of the dynamic fracture tests performed on the A441 steel is that the data obtained by Madison and Luft agree within data scatter with the K_c values resulting from this program. The results of the present program appear, however, to show less scatter and tend to correspond to the lower portion of the scatter band of Madison-Luft data.

Similar dynamic fracture tests were performed on the RQ-100B steel and, because of its high degree of toughness in the region above -40° F, most of the K_c values resulted from the thickness reduction technique. A delay arose in the testing of this material due to a dynamometer failure in the Vibrophore, the high frequency pre-cracking machine, and for this reason only a limited number of tests were completed.

In the results for both structural steels it was evident that, for values of $r_Y > 1/4$ in., the computed K_c values showed increased variation. In this testing region the net section of the specimen is approaching a general yielding condition. In addition onset of rapid fracturing tends to occur on the rising portion of the R-curve. Both circumstances would tend to cause some increase of data scatter.

Most of the testing emphasis was concentrated on testing conditions such that the net section was near or beyond a condition of general yielding. The primary effort of the program for this region consisted in use of a thickness reduction to evaluate K_c. Thickness reduction measurements were made on the broken halves of the test specimens at the two measurement positions, as discussed previously, and from these measurements "equilibrium" positions were found using the empirical thickness reduction technique for each of the measurement positions. Equating the crack opening stretch to the thickness reduction at each of these two equilibrium positions two corresponding K_c values were calculated from these δ values. The two K_c resultants were averaged and plotted in the graphs of Figs. 18 to 22.

The graphs resulting from the thickness reduction computations show a plausible variation of fracture toughness with temperature. This method results in a sharper increase in the resulting K_c values than does the procedure based upon measurements of maximum load. This is expected in the region of general yielding where the deformations in in the test specimen become very pronounced and the fracture toughness accordingly high. It is also observed that in the region of overlapping data that the thickness reduction results for K_c lie above those obtained using linear elastic fracture mechanics. This is desirable because, in the thickness reduction procedure, the plateau or maximum K value, corresponding to the shelf of an R-curve, is being measured. This plateau value of K or "effective" K_c value is somewhat higher than the critical K value which corresponds to the initiation of unstable

crack growth in the test specimen and which is the K level computed from maximum load measurements. The difference between K_c and the plateau value of K depends on the test conditions and the resulting state of stress. The difference is minimal and very close to zero in a K_{Ic} or plane strain type test while it is significant in the region of general yielding.

The one graph, Fig. 25, presenting the results of the bend-angle investigation on A514 - 2" plate gives some assurance that this measurement technique is plausible. The two data points for each of the temperatures, -7^{o} F and 72^{o} F, represent the bend-angle technique, and the two points correspond to λ values of 0 and 1, with $\lambda = 1$ resulting in the higher values of an "effective" K_c. The results seem to indicate that λ should lie between these two extremes to produce reasonable "effective" K_c values.

As a check on the thickness reduction technique it would have been desirable to investigate another plasticity concept in formulating a similar fracture toughness characterization method beyond general yielding so that the results of both methods could be checked for similarity. One such technique is the bend-angle approach described in this report. Several dynamic fracture tests of double-sized test specimens could also be conducted in order to extend the range of applicability of the linear elastic solution into an area which contained only plasticity K_c values beforehand. This would be done both as another check on the thickness reduction method and as an alternative procedure for toughness evaluation.

The results from the thickness reduction method agree satisfactorily with the maximum load K_c data where the two methods overlap. However, in the region of gross general yielding the accuracy of this technique is questionable since it was not checked with the results of any accurate K_c measurement technique. For this reason it is suggested that future research involving the bend-angle concept and the double-sized test specimens be undertaken so that the uncertainities of these plasticity techniques in the region of gross general yielding can be investigated and corrected if they are found to exist. In this way a fracture toughness characterization method will be available to calculate K_c over the entire spectrum of stress conditions existing ahead of the crack from the plane strain mode of failure to the condition of gross general yielding.

5. CONCLUSIONS

As a result of the work performed in this program it is concluded that:

1. The drop weight tear test procedure is a useful measurement procedure for obtaining dynamic values of K_c.

2. The oscillations appearing in the load-time records are a result of reflected compressive-tensile wave motion in the drop-weight. They have no effect on the maximum load which is used to compute K_c.

3. The best method of cushioning the rate of load application onto the test specimen is to use half-round cushions of unhardened tool steel. With the use of these cushions the resulting loading times are 0.5 to 1.5 milliseconds.

4. The RQ-100B structural steel is much tougher than the A441 steel with the curve of K_c versus temperature for the RQ-100B steel having a steeper slope in the transition range.

5. The thickness reduction technique for measuring K_c results in reasonable values of toughness for both steels.

6. The preliminary studies in the bend-angle procedure for computing K_c shows good promise.

6. ACKNOWLEDGMENTS

This report presents the results of Project 366 entitled the "Application of Fracture Mechanics to Structural Steels" conducted at Fritz Engineering Laboratory of Lehigh University, Bethlehem, Pennsylvania. Dr. D. A. VanHorn in Chairman of the Department of Civil Engineering, and Dr. L. S. Beedle is Director of the Laboratory.

The director of the project was Dr. G. R. Irwin Professor of Lehigh University. The project was sponsored by the Bethlehem Steel Corporation, and appreciation goes to Mr. James Scott and Mr. Michael Healey for their assistance in the program. The aid rendered by Dr. Roger Slutter of Fritz Engineering Laboratory is also acknowledged.

The author would also like to thank Mr. Kenneth Harpel, Superintendent of Fritz Engineering Laboratory, and his staff; Mr. Hugh Sutherland, Instruments Associate, for his assistance in the instrumentation; and Mr. John Gera and Mrs. Sharon Balogh, draftsmen. Special thanks are due to Mrs. Dorothy Fielding who typed and aided in the preparation of this report.

8. NOMENCLATURE

a	effective crack length, in.
a_F	increment of crack grown in fast fatigue, in., Fig. 7
a_o	initial crack length, in.
a_s	increment of crack grown in slow fatigue, in., Fig. 7
a_{ST}	increment of stable crack growth, in.
A_w, A_o, A_1	coefficients depending on the ratio of span length to beam depth, Eq.11
B	specimen thickness, in.
B'	reduced specimen thickness, in.
C	compliance of the specimen, in./lb.
D	distance of travel for reflected waves, in., Fig. 24
E	uniaxial tensile (Young's) modulus, psi
G	shear modulus, psi
$\mathscr{G}$	strain energy release rate, in-lb/in.^{2}
$\mathscr{G}_{max}$	maximum strain energy release rate, in-lb/in.^{2}
K	stress intensity factor, ksi $\sqrt{in}$
K_c	critical stress intensity factor, ksi $\sqrt{in}$
K_I	stress intensity factor for opening mode of crack surface displacement (Mode I) ksi $\sqrt{in}$
K_{Ic}	critical stress intensity factor for opening mode of crack surface displacement (Mode I) ksi $\sqrt{in}$
K_M	maximum stress intensity factor corresponding to plateau value of resistance curve, ksi $\sqrt{in}$

K_{min}	minimum stress intensity factor for particular test conditions, ksi $\sqrt{in.}$
K_R	stress intensity factor corresponding to the values of the resistance curve, ksi $\sqrt{in.}$
K'	stiffness of the specimen, lb/in.
L	specimen's support length for dynamic fracture test, in.
L_F	specimen's support length for fatigue crack growth, in., Fig. 7
L_{Lig}	"weighted" length of ligament remaining intact in partially fractured specimen, in.
M	bending moment (per unit thickness) on specimen, kip-in/in.
M'	mass of drop-weight, lb-sec^2/in.
n	work hardening exponent, assumed equal to uniform elongation strain in a tensile test
P	applied load on specimen, kip
P_c	critical load on specimen for crack instability, kip
P_{max}	maximum load on specimen during fatigue process, kip
Q	arbitrary constant, Fig. 16
r	radial position coordinate measured from leading edge of the crack, in., Fig. 1
r_Y	plasticity correction factor, in.
r^A_Y	assumed plasticity correction factor in computer program, in., Fig. 17
r^C_Y	calculated plasticity correction factor in computer program, in., Fig. 17
S, S_o, S_n	thickness-reduction measurement position perpendicular to brittle or flat portion of fracture surface, in.

t	loading time to point of fracture, sec.
T	temperature, ^{o}F
T'	period of reflected waves, sec., Fig. 24
V	velocity of reflected waves, in/sec., Fig. 24
v	displacements normal to and close to the crack plane, in., Fig. 1
W	specimen depth, in.
X_1, X_2	measurement readings along edge of slice
Y	dimensionless ratio relating stress intensity factor to crack length
α	angle of taper of the 90^{o} Chevron notch
β	bend-angle of a partially fractured specimen
δ	crack opening stretch, in., Fig. 1
θ	angular position coordinate measured from the apparent leading edge of the crack, Fig. 1
λ	arbitrary constant which preliminary experiments show to be between 0 and 1
μ	Poisson's ratio
π	
ρ	material mass density, kip-sec^2/in.^{4}
σ	nominal tensile stress on gross section, ksi
σ_f	maximum stress in the specimen using simple beam theory, ignoring the crack, ksi, Eq. (A2.4)
σ_M	maximum stress in the specimen using simple beam theory, considering the portion of the cracked section not occupied by the crack, ksi
σ_{max}	nominal tensile stress on gross section at the point of instability of crack extension, ksi, Fig. 3

σ_{YS} uniaxial tensile yield stress (yield point), ksi

σ_x tensile stress component parallel to the plane of a crack in the x-coordinate direction, ksi

σ_y tensile stress component normal to the plane of a crack in the y-doordinate direction, ksi

σ_z tensile stress component parallel to the leading edge of the crack in the z-coordinate direction, ksi

τ_{xy} shearing stress in the y-coordinate direction on a plane perpendicular to the x-coordinate, ksi

APPENDIX 1

SAMPLE K_c CALCULATION FROM THICKNESS-REDUCTION MEASUREMENTS

A441 Steel - 1 inch thickness, 36.5° F B = 0.9502 in.

$$S_o = \frac{B}{9} = 0.1056 \text{ in.}$$

$$r_Y = \frac{E\,\delta}{2\pi\,\sigma_Y} = 62.82$$

S	X_1	X	B'	δ
0.110	1.0144	1.9624	0.9480	0.0022
0.105	1.0146	1.9622	0.9476	0.0026
0.100	1.0147	1.9618	0.9471	0.0031
0.095	1.0149	1.9615	0.9466	0.0036

	S_n	δ	r_Y	r_Y/B	f
1	0.1056	0.00255	0.1602	0.1690	0.3034
2	0.0991	0.00349	0.2192	0.231	0.3129
	0.0991	0.00318	0.2004	0.211	0.3103
	0.0983	0.00327	0.2054	0.216	0.3110
	0.0985	0.00325	0.2042	0.215	0.3108
	0.0984				

$$K_M = \sigma_{YS}\sqrt{2\pi}\,r_Y = 86.0 \text{ ksi } \sqrt{\text{in}}$$

K_c = 71.0 ksi $\sqrt{\text{in}}$ (calculated from maximum load)

Note: S, S_n, X_1, X_2, B', δ, r_Y → in.

APPENDIX 2

LIMITATIONS IN THE LINEAR ELASTIC APPROACH TO FRACTURE MECHANICS DUE TO SPECIMEN SIZE

For A441 steel, if the plastic zone is small enough so that the 1 inch and 2 inch thick test specimens satisfy the size requirements for the tentative ASTM K_{Ic} method, then the K_c value must be less than 51 ksi $\sqrt{in}$ for the dynamic tests. This estimate assumes σ_{YS} (dynamic) is 80 ksi and employs the equation

$$\left(\frac{K}{\sigma_{YS}}\right)^2 \leq 0.4\ a = 0.4 \text{ in.} \qquad \text{(A2.1)}$$

With the A441 steel and at the temperatures of principle interest, the K_c values lie above the one given in the preceding paragraph. Thus in the tests of main interest to this project, resistance to onset of rapid fracturing is assisted by appreciable amounts of thickness reduction type yielding and, for analysis consistency, the K_c values include a plasticity correction. In other words, the visual or actual crack size, a_o, is augmented by the amount r_Y, given previously in Eq. (7). In equation form

$$a = a_o + r_Y \qquad \text{(A2.2)}$$

As the ratio of r_Y to the crack depth, a_o, increases beyond 1/10, the stress intensity factor interpretation of K becomes increasingly inaccurate.[6] Nevertheless, as explained in Ref. 6

the r_Y corrected K values retain physical significance in this range in terms of a close relationship between K^2 and plastic strain magnitudes near the leading edge of the crack. It is necessary, however, to recognize the region of K values corresponding to initial development of general yielding in order to establish a sensible limit for applicability of the r_Y corrected K value calculation method.

For a notched-bend test specimen the equation for calculation of K can be written in the form

$$K = \sigma_f \sqrt{a}\ Y\ (\frac{a}{W}) \qquad \text{(A2.3)}$$

where the function $Y(a/W)$ is available from numerical studies in the form of a power series truncated to the first 5 terms.[8] The power series form of $Y(a/W)$ applicable to the Lehigh test specimen requires a moderate extrapolation of results given by Ref. 8. This adjustment was discussed and verified by experimental calibration in Ref. 4.

σ_f is given by $6M/W^2$ where M is the bending moment (per unit thickness) applied to the section containing the crack. In other words σ_f is the simple beam theory maximum stress ignoring the crack. If the same analysis is applied to the portion of this section not occupied by the crack, the maximum stress, σ_M, is given by

$$\sigma_M = \sigma_f\ (1 - \frac{a_o}{W})^{-2} \qquad \text{(A2.4)}$$

If a is assumed to be 1.4 inches and σ_M, is at the dynamic yield point, 80 ksi, the value of K is 58 ksi $\sqrt{\text{in.}}$ If a is still assumed to be 1.4 inches and σ_M is 1.5 times 80 ksi, the value of K is 115 ksi $\sqrt{\text{in.}}$

The second of these estimates corresponds to assuming the bending moment (per unit thickness) is given by the (perfectly) plastic behavior equation

$$M = \frac{1}{4} \sigma_{YS} (W - a_o)^2 \qquad \text{(A2.5)}$$

or

$$M = \frac{1}{6} (1.5 \sigma_{YS}) (W - a_o)^2 \qquad \text{(A2.6)}$$

where σ_{YS} = 80 ksi. Bearing in mind that constraint and work hardening would tend to elevate the resistance to plastic deformation, these estimates suggest that the limit of applicability of the r_Y corrected K method must lie in the upper part of the range from 58 ksi $\sqrt{in.}$ to 115 ksi $\sqrt{in.}$

An alternative method for estimating the above limit is to assume

$$2r_Y = \frac{2}{3} \left(\frac{W - a_o}{2} \right) \qquad \text{(A2.7)}$$

This procedure is based upon comparisons to solutions for the problem of a central crack in a finite width plate. For this problem, assuming $2a_o = W/2$ and the equation

$$K^2 = \sigma^2 \pi a \sec \left(\frac{\pi a}{W}\right) \qquad \text{(A2.8)}$$

one finds that the average stress on the net section is equal to σ_{YS} when

$$2r_Y = \frac{2}{3} \left(\frac{W}{4}\right) \qquad \text{(A2.9)}$$

In applying this result to the notched-bend test, the net ligament, W/4 in Eq. (A2.9), is replaced in Eq. (A2.7) by the distance from the crack tip to the neutral axis, $(W - a_o)/2$. Equation (A2.7) provides 108 ksi $\sqrt{in}$ as an estimate of the K value calculation limit. When Eq. (A2.9) is derived using values of $2a_o$, less than W/2, the coefficient of the net ligament in Eq. (A2.9) is decreased and such estimates would lead to estimates of the calculation limit as small as 95 ksi $\sqrt{in}$.

From the preceding discussion, dynamic K_c values obtained for the A441 steel which are below 100 ksi $\sqrt{in}$ can be used without serious problems of interpretation, while K_c values above 110 ksi $\sqrt{in}$ are probably too large for validity of the calculation method. For the RQ-100B steel, the estimates of K value calculation limits should be increased in proportion to the increased size of the dynamic yield strength of RQ-100B.

Table 1 Material Properties of Plates

Mechanical Properties

	Plate Thickness(in)	Yield Strength(psi)	Tensile Strength(psi)	% Elongation
A441	1/2	56,650	83,050	27.2 in 4"
	1	55,900	82,300	
	2	55,000	87,000	29.0 in 2"
RQ-100B	1/2	86,575	111,452	23.5 in 2"
	1	84,075	101,090	24.5 in 2"
	2	81,105	97,125	26.0 in 2"

Chemical Properties*

	C	Mn	P	S	Si	Cu	Cr	Ni	Mo	V	B
A441	.20	1.08	.017	.025	.21	.23	.03	.02	.002	.051	--
RQ-100B	.16	.69	.011	.025	.26	--	.04	1.37	.59	--	.003

*The chemical properties presented are representative of the 1/2" plate. Those for the 1" and 2" plates may differ moderately.

Table 2 Dynamic K_c Results

A441, B = 1/2 in., Dynamic Loading

Spec. No.	Max. Load (kips)	B (in.)	Temp. (°F)	σ_{YS} (ksi)	K_c Maximum Load (ksi $\sqrt{in}$)	K_c Thickness Reduction at B/2 (ksi$\sqrt{in}$)	K_c Thickness Reduction at 3B/4 (ksi$\sqrt{in}$)	K_c Thickness Reduction Avg. (ksi$\sqrt{in}$)
A023	26.25	0.492	83.0	74.9	> 145	-	-	-
A024	27.50	0.492	83.0	73.2	> 145	-	-	-
A025	12.00	0.493	- 8.0	84.6	61.3	-	-	-
A026	14.50	0.486	- 8.0	84.0	79.6	-	-	-
A029	18.00	0.483	32.0	78.7	124.6	187.7	163.5	150.6
A030	22.00	0.476	32.0	78.7	> 145	-	-	-
A031	18.50	0.482	14.0	81.0	126.1	120.9	125.9	123.4
A032	17.50	0.476	14.0	81.0	112.8	122.1	129.9	126.0

Table 2 Dynamic K_c Results (continued)

A441, B = 1 in., Dynamic Loading

Spec. No.	Max. Load (kips)	B (in.)	Temp. (^{o}F)	σ_{YS} (ksi)	K_c Maximum Load (ksi$\sqrt{in}$)	K_c Thickness Reduction at B/2 (ksi$\sqrt{in}$)	K_c Thickness Reduction at3B/4 (ksi$\sqrt{in}$)	K_c Thickness Reduction Avg. (ksi$\sqrt{in}$)
A114	30.00	0.935	154.0	69.8	> 125	435.9	450.8	443.4
A119	33.00	0.964	81.0	73.6	> 125	-	-	-
A120	24.50	0.970	81.0	73.5	> 125	-	-	-
A121	20.00	0.971	32.0	78.2	73.9	78.1	84.5	81.3
A122	20.00	0.970	32.0	78.3	75.4	-	-	-
A124	11.25	0.977	-80.5	92.1	39.4	-	-	-
A125	15.00	0.976	7.7	79.3	51.0	-	-	-
A126	13.25	0.974	-35.5	91.7	45.2	-	-	-
A127	12.50	0.936	-44.5	86.7	43.3	-	-	-
A128	15.75	0.971	7.7	79.0	55.1	-	-	-
A129	15.38	0.955	7.7	79.1	55.1	-	-	-
A131	9.50	0.967	-62.5	91.5	32.4	-	-	-
A134	24.00	0.971	72.0	73.5	111.3	-	-	-
A135	21.00	0.977	72.0	73.0	83.8	-	-	-
A139	25.50	0.967	72.0	71.9	> 125	-	-	-
A140	25.50	0.961	72.0	71.9	> 125	-	-	-
A142	19.00	0.950	36.5	76.0	71.0	-	-	-
A143	30.00	0.968	72.0	72.5	> 125	-	-	-
A144	26.50	0.978	72.0	72.7	> 125	-	-	-
A145	23.00	0.957	72.0	73.5	104.7	218.5	246.4	232.5
A146	22.50	0.948	72.0	74.1	105.4	-	-	-
A147	20.00	0.982	72.0	77.8	73.8	-	-	-
A149	26.00	0.985	72.0	72.4	> 125	-	-	-
A150	16.50	0.964	72.0	75.8	71.0	-	-	-
A153	18.50	0.960	72.0	77.8	67.8	-	-	-

Table 2 Dynamic K_c Results (continued)

A441, B = 2 in., Dynamic Loading

Spec. No.	Max. Load (kips)	B (in.)	Temp. (°F)	σ_{YS} (ksi)	K_c Maximum Load (ksi√in)	K_c Thickness Reduction at B/2 (ksi√in)	K_c Thickness Reduction at 3B/4 (ksi√in)	K_c Thickness Reduction Avg. (ksi√in)
A223	36.50	1.956	83.0	73.2	102.7	-	-	-
A224	36.50	1.956	83.0	73.2	102.8	-	-	-
A225	21.00	1.955	- 5.8	83.2	48.1	-	-	-
A226	21.00	1.955	- 5.8	83.2	48.3	-	-	-
A229	55.00	1.958	188.0	67.5	> 119	267.3	-	267.3
A230	52.50	1.942	160.0	69.9	> 119	237.0	-	237.0
A231	36.90	1.946	77.0	73.8	> 119	110.6	-	110.6
A232	36.25	1.939	77.0	73.8	> 119	83.9	-	83.9

Table 2 Dynamic K_c Results (continued)

RQ-100B, B = 1/2 in., Dynamic Loading

Spec. No.	Max. Load (kips)	B (in.)	Temp. (^{o}F)	σ_{YS} (ksi)	K_c Maximum Load (ksi$\sqrt{in}$)	K_c Thickness Reduction at B/2 (ksi$\sqrt{in}$)	K_c Thickness Reduction at 3B/4 (ksi$\sqrt{in}$)	K_c Thickness Reduction Avg. (ksi$\sqrt{in}$)
B04	41.25	0.533	- 12.0	108.8	> 211	335.6	366.7	351.2
B06	38.75	0.525	- 12.0	109.0	> 211	362.0	382.6	372.6
B07	38.75	0.525	- 12.0	109.1	> 211	-	-	-
B011	15.00	0.522	- 92.0	122.8	76.7	56.9	53.3	55.1
B012	15.50	0.525	- 92.0	123.1	79.3	53.3	53.3	53.3
B013	29.40	0.510	- 53.0	115.8	> 211	220.5	238.7	229.6
B014	27.50	0.510	- 53.0	115.8	> 211	155.5	157.2	156.4
B016	32.50	0.515	- 16.0	111.1	> 211	293.3	330.5	321.9
RQ-100B, B = 1 in., Dynamic Loading								
B11	32.50	0.939	- 90.0	126.5	94.1	-	-	-
B12	27.50	0.962	- 90.0	124.4	75.8	54.6	72.3	63.5
B15	55.00	0.940	- 12.0	110.8	> 206	347.8	437.5	392.7
B17	31.25	0.959	- 92.0	121.5	> 206	131.4	129.1	130.3
B18	43.75	0.935	- 53.0	115.0	90.9	189.4	244.2	216.8
B110	67.50	0.958	- 16.0	109.3	149.7	403.3	423.1	413.2
B111	52.50	0.936	- 53.0	113.7	> 206	306.2	322.9	314.6
RQ-100B, B = 2 in., Dynamic Loading								
B23	57.50	2.022	- 90.0	125.0	89.1	-	-	-
B25	80.00	198.4	- 53.0	113.3	145.9	-	-	-

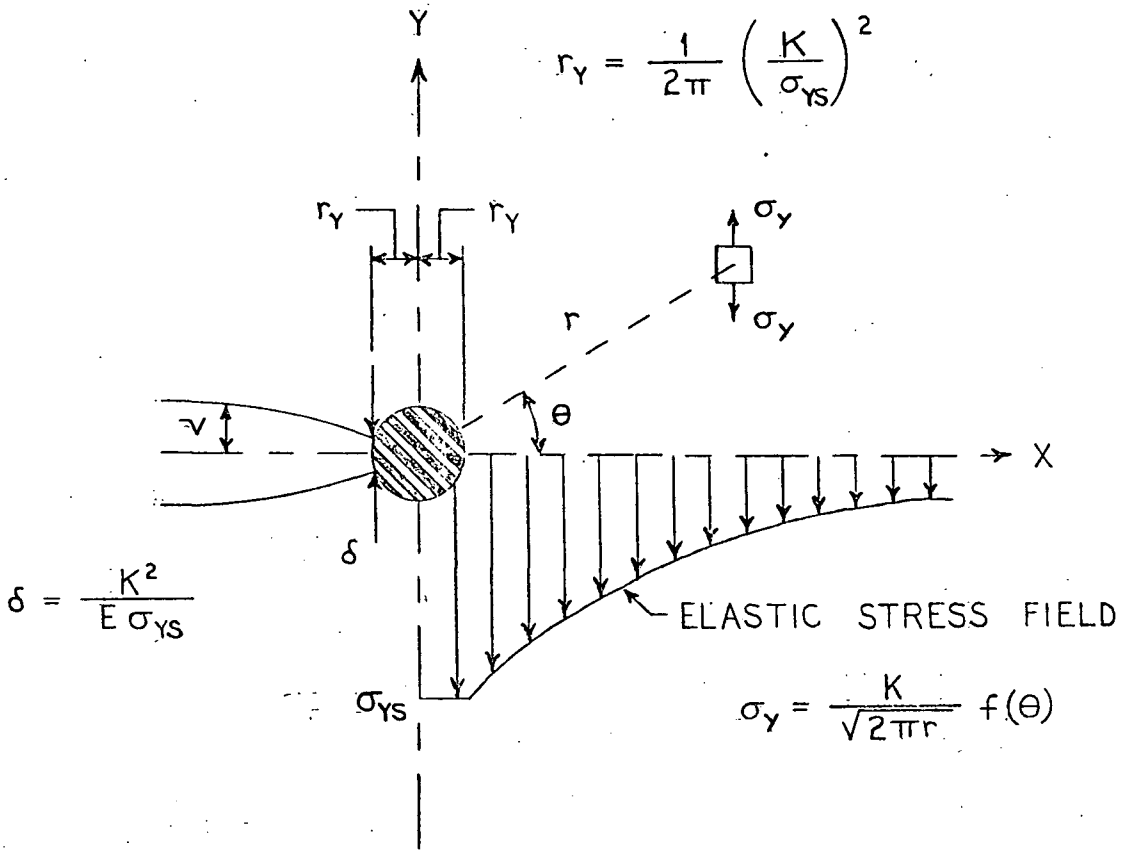

Fig. 1 Leading Edge of a Crack

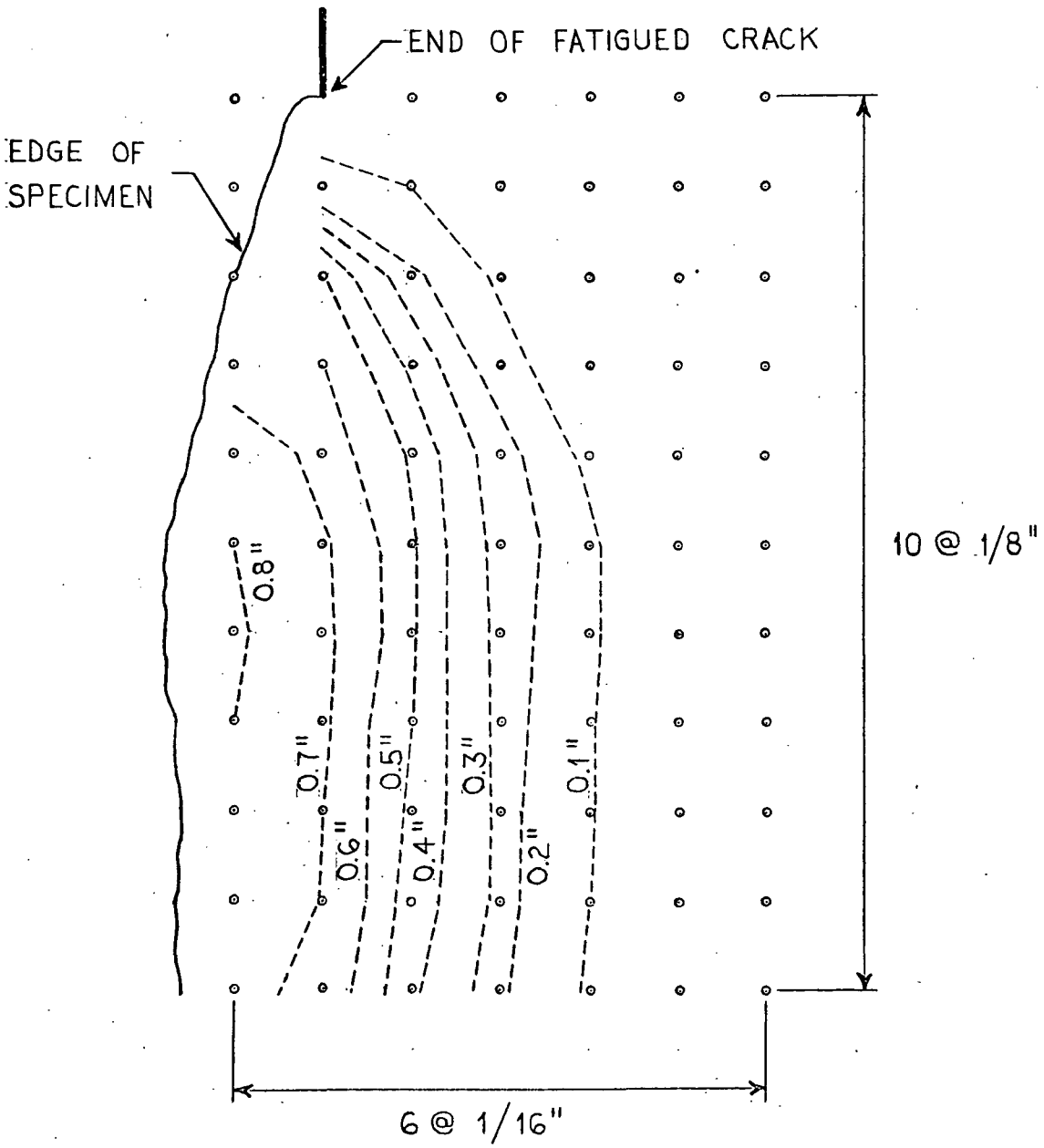

Fig. 2 Thickness Reduction Grid

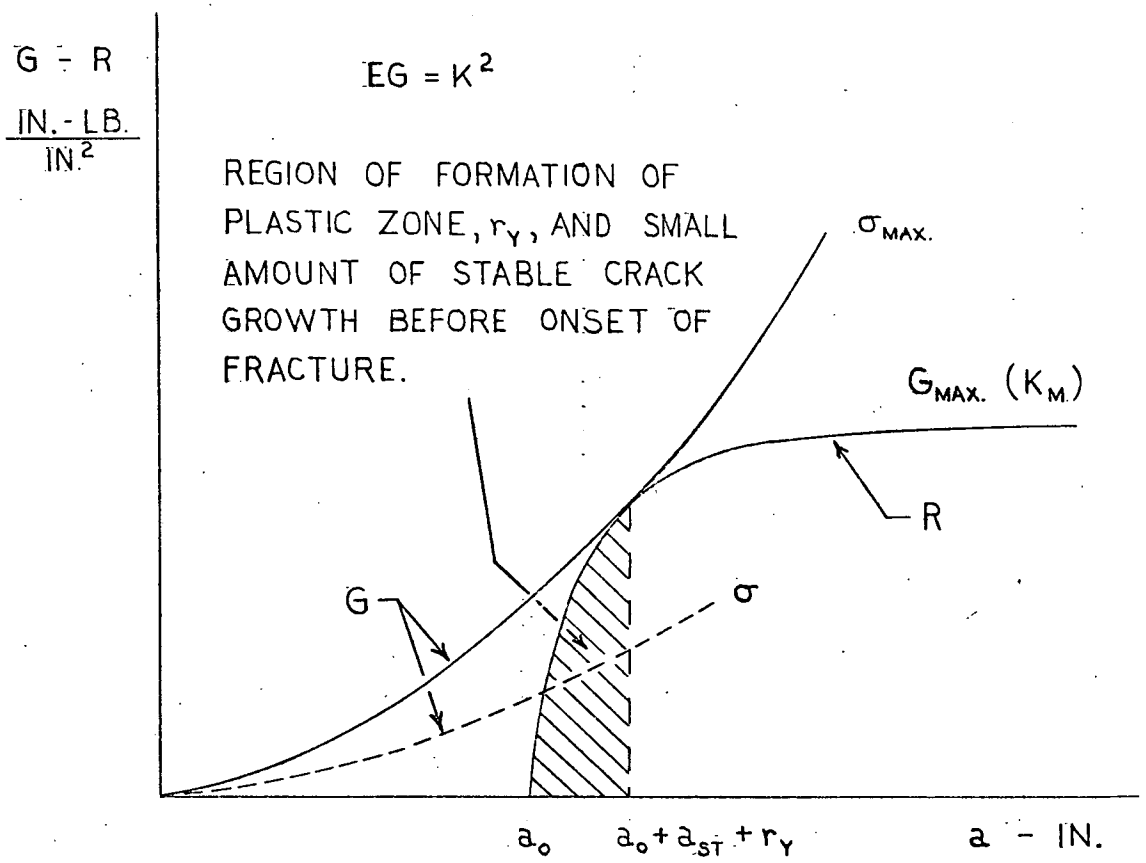

Fig. 3 Representation of the Crack Extension Instability Condition as a Tangency Between the G- and R-Curves

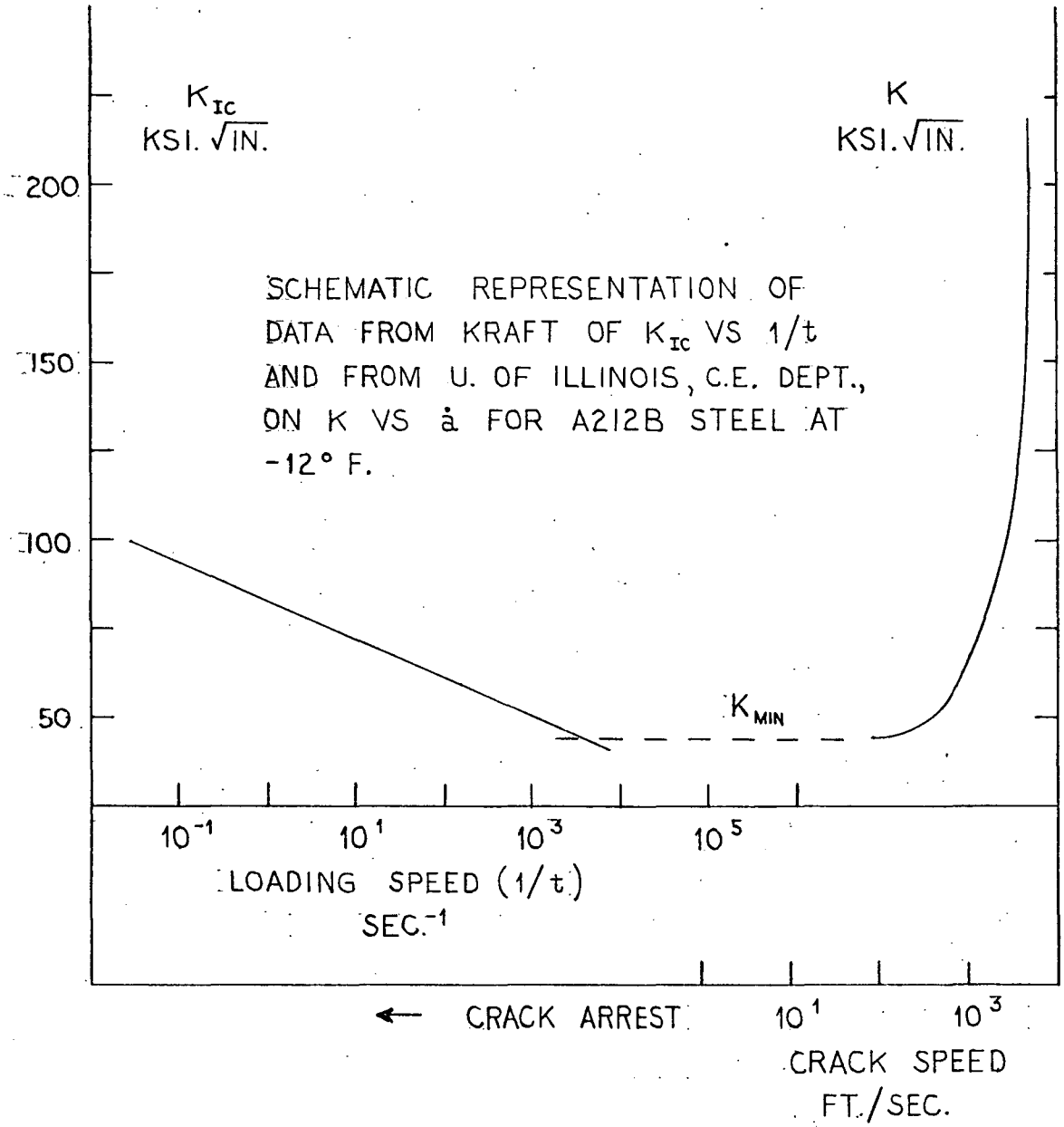

Fig. 4 Relationship of K_{Ic} vs Loading Speed and K_c vs Crack Speed

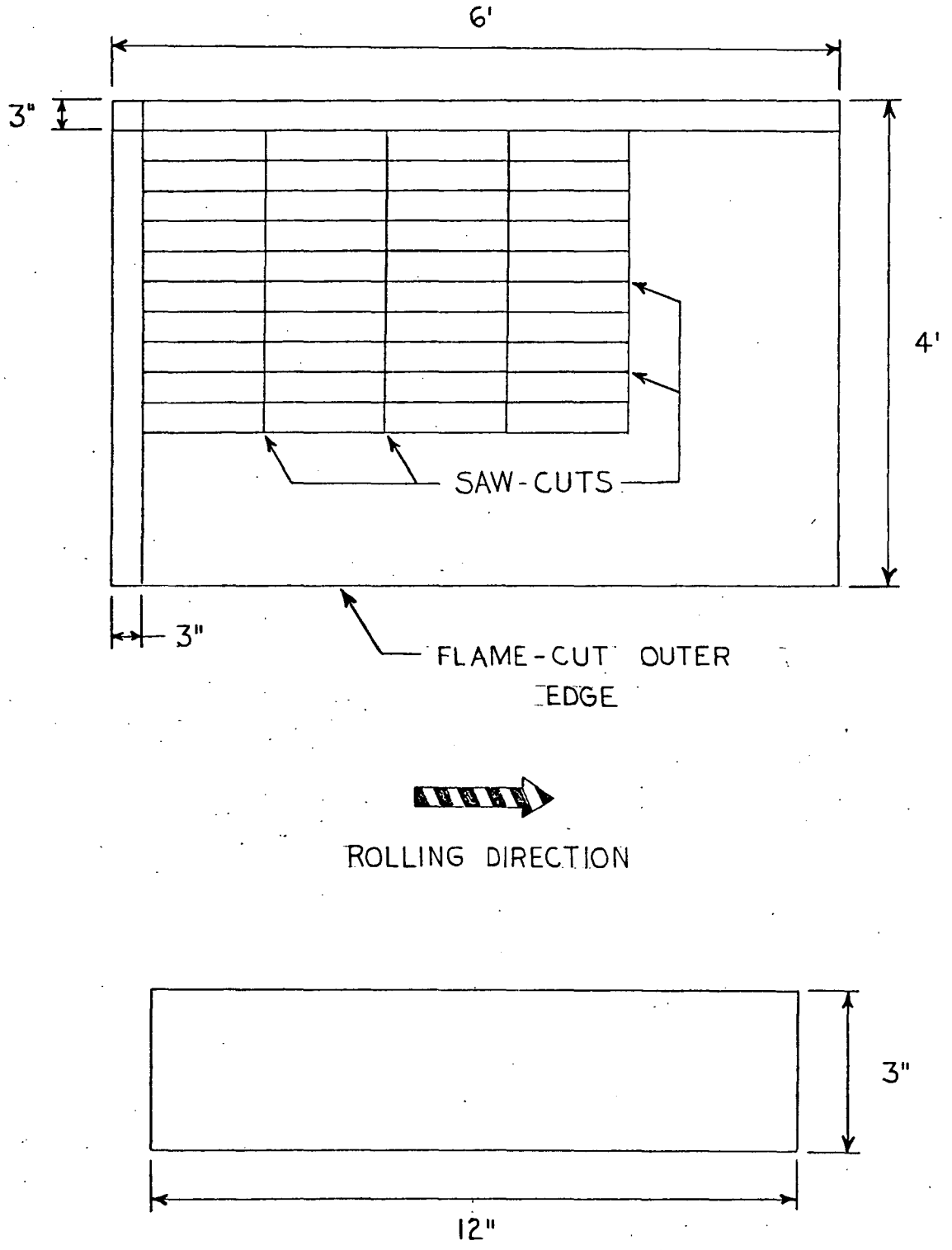

Fig. 5 Specimen Orientation in Rolled Plate

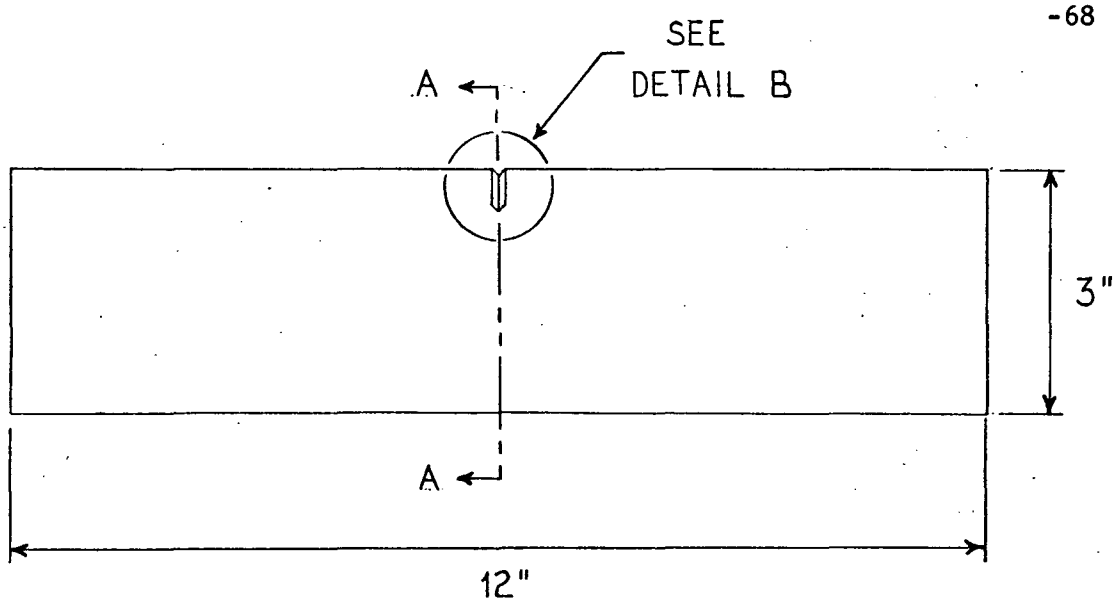

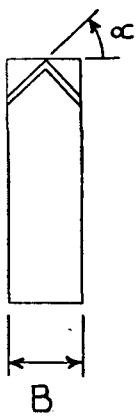

B = PLATE THICKNESS	α
$\frac{1}{2}$"	45°
1"	45°
2"	29°

SECTION A-A

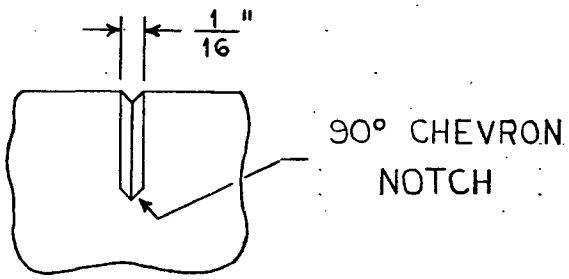

DETAIL B

Fig. 6 Lehigh Test Specimen

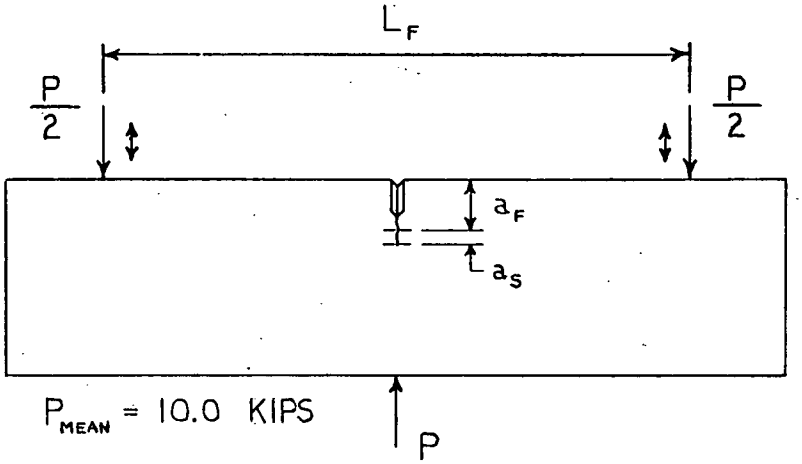

A441 STRUCTURAL STEEL

GROWTH RATE		PLATE THICKNESS		
		1/2"	1"	2"
FAST	$P_{MAX.}$	15.0	20.0	20.0
	L_F	7.0	9.5	11.0
	a_F	0.5	0.8	1.15
	$CYCLES_{AVG.}$	189,000	69,000	192,000
	K_C	46.8	57.0	42.8
SLOW	$P_{MAX.}$	12.6	13.4	14.7
	L_F	7.0	9.5	11.0
	a_S	0.1	0.2	0.1
	$CYCLES_{AVG.}$	178,000	277,000	162,000
	K_C	42.7	43.9	33.8

NOTE : $P_{MAX.} \rightarrow$ KIPS
$L_F, a_F, a_S \rightarrow$ IN.
$K_C \rightarrow$ KSI.$\sqrt{IN.}$

Fig. 7 Fatigue Pre-Cracking Loading Configuration and Data for A441 Plates

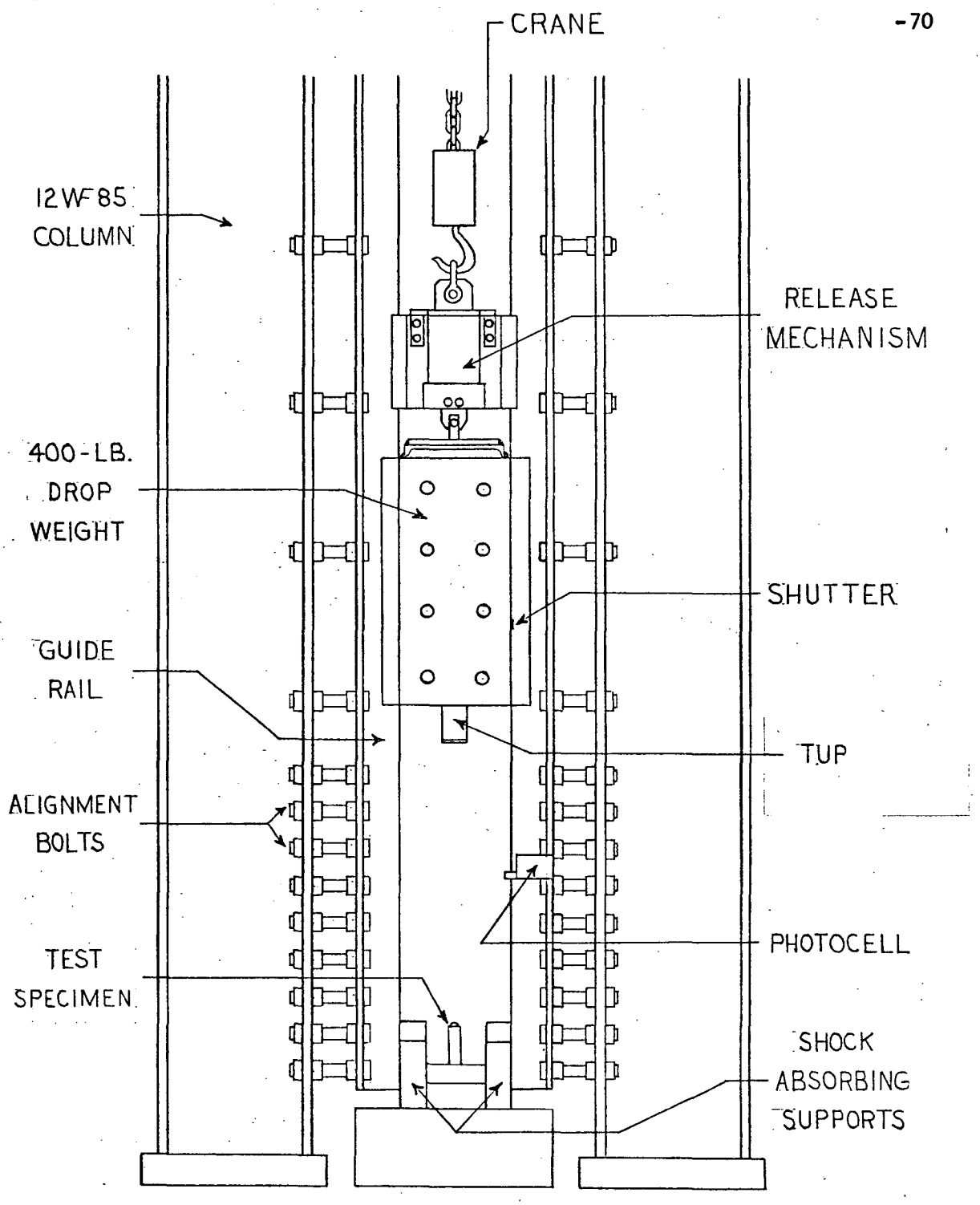

Fig. 8 Lehigh Drop-Weight Tear Test Machine

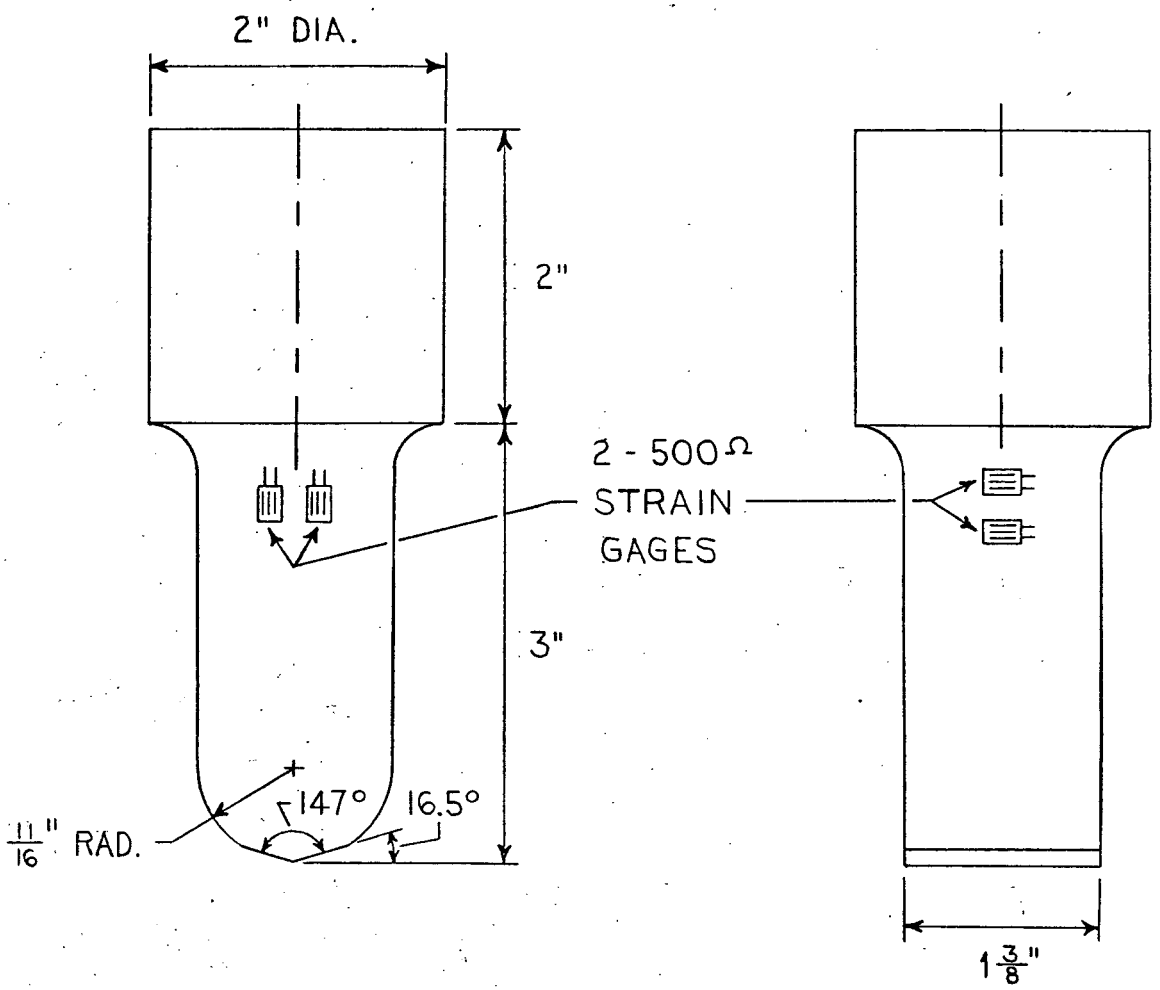

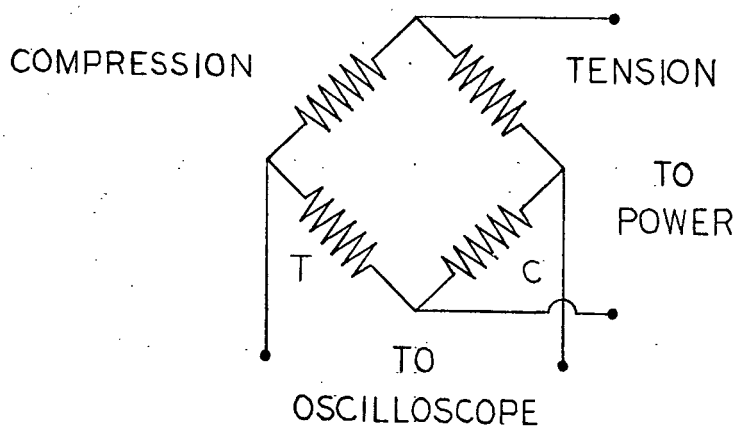

Fig. 9 Load Dynamometer (Tup)

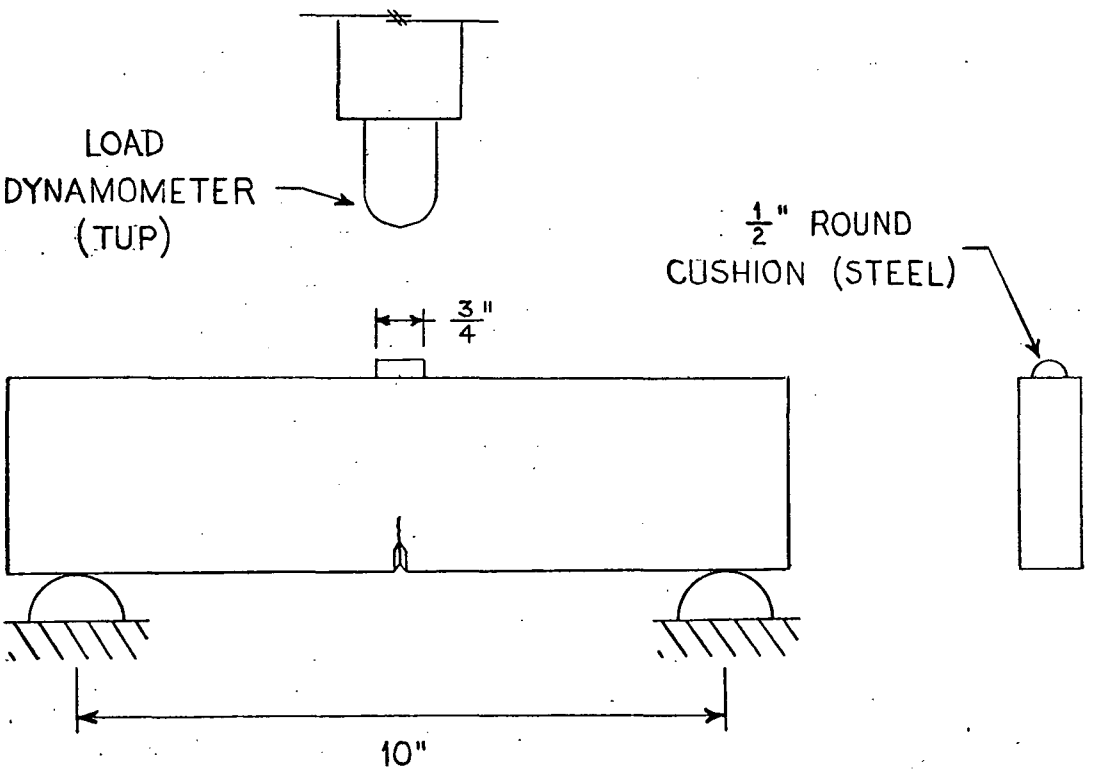

Fig. 10 Padded Test Specimen on Test Fixture

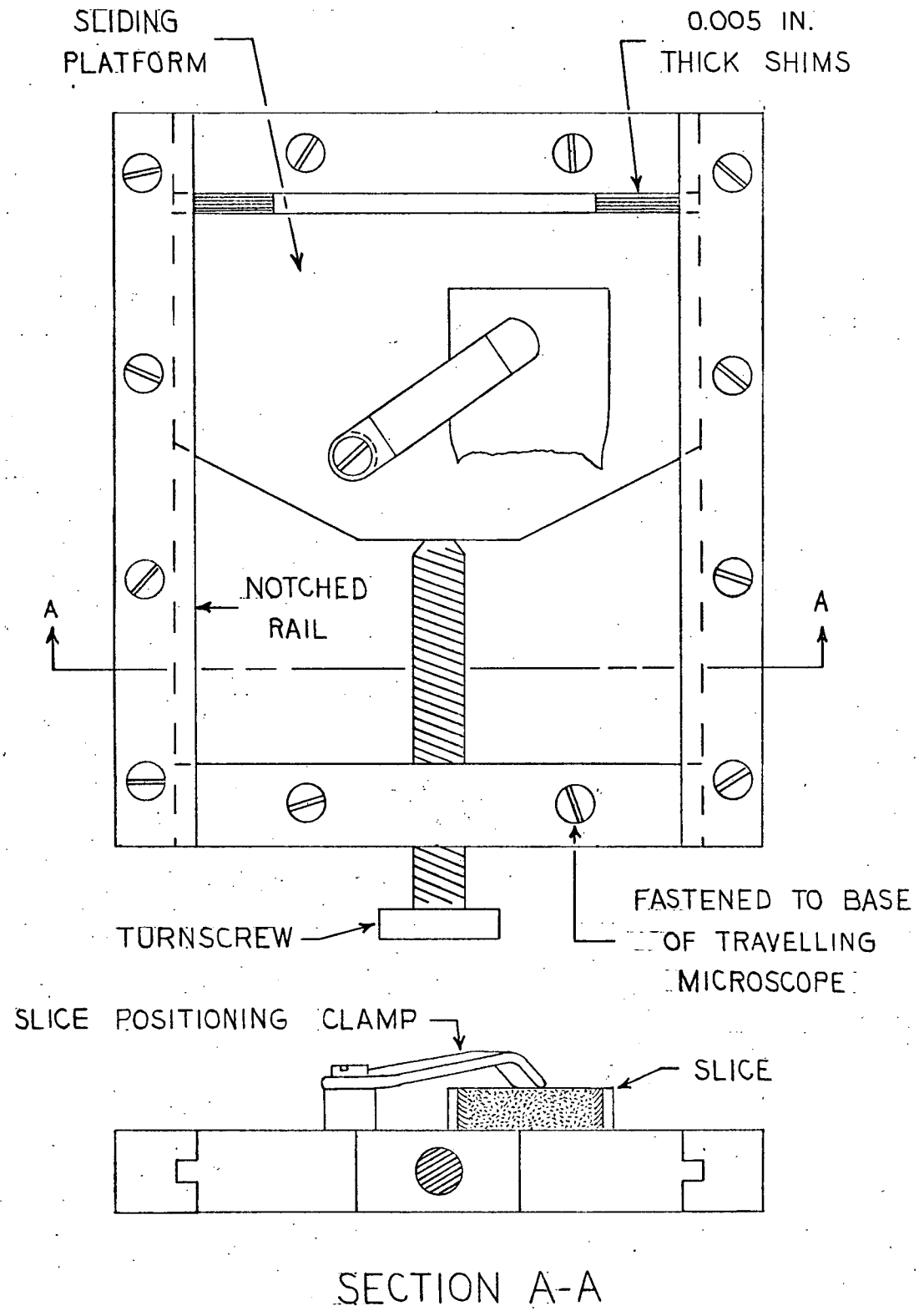

Fig. 11 Shimming Assemglage

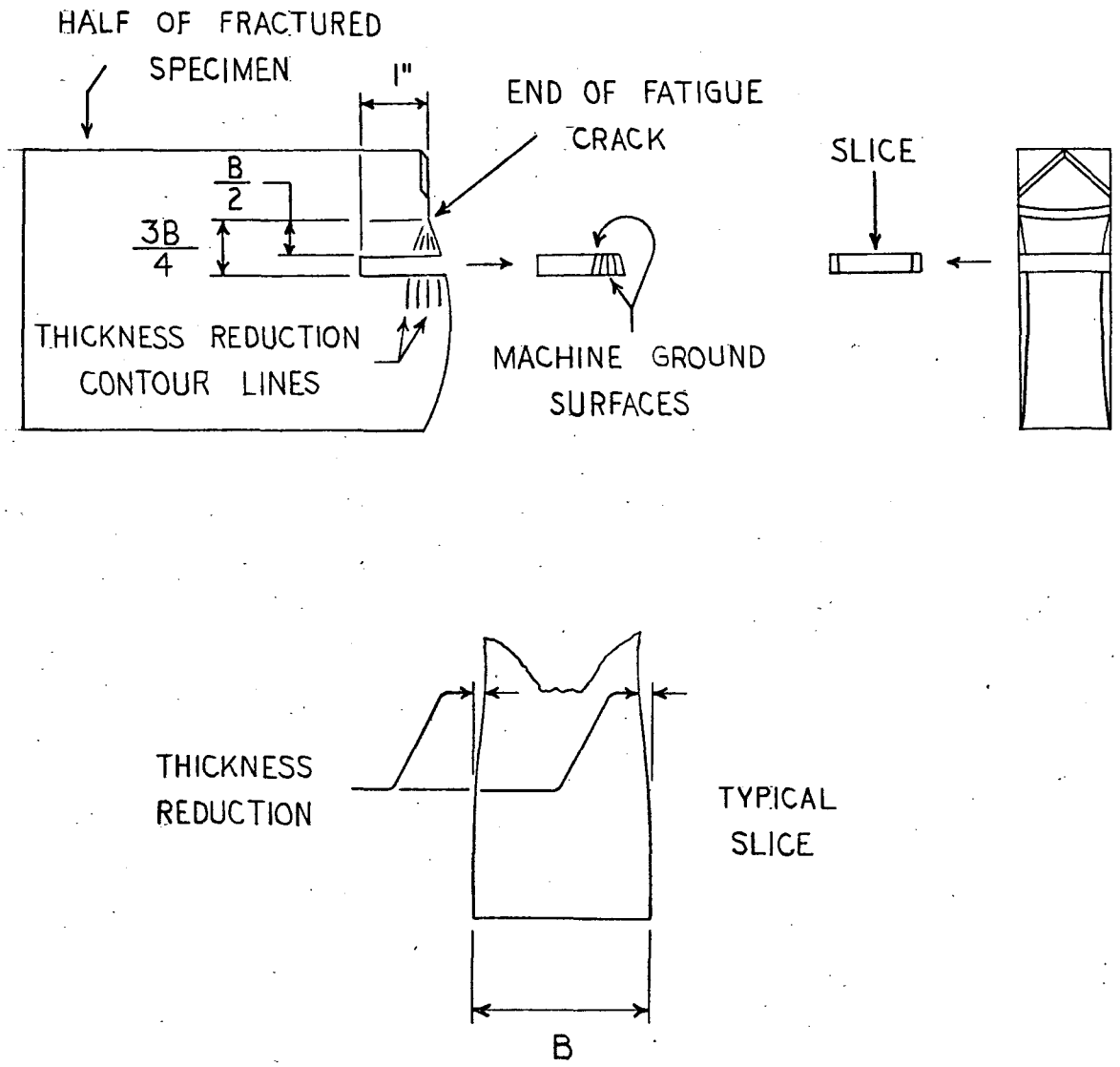

Fig. 12 Slicing Technique Employed in Thickness Reduction Procedure

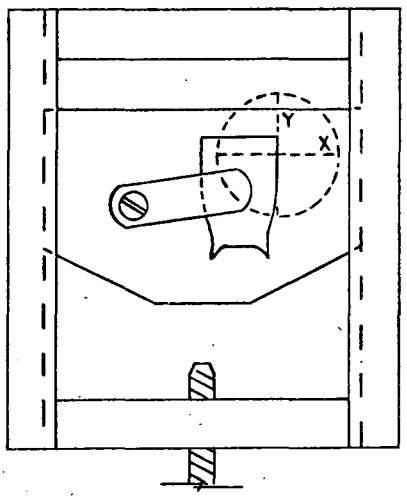

(1) POSITION EDGE OF SLICE PARALLEL TO Y-DIRECTION CROSSHAIR.

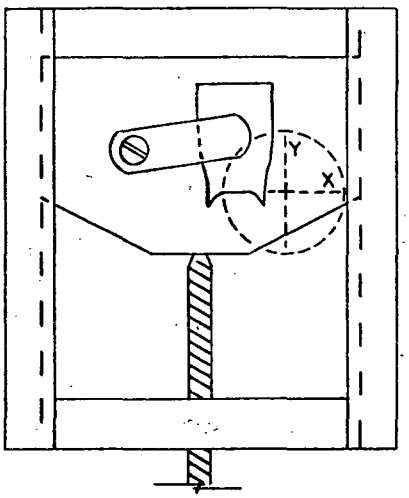

(2) POSITION X-DIRECTION CROSSHAIR PARALLEL TO BRITTLE PORTION OF FRACTURE SURFACE (ZERO POSITION).

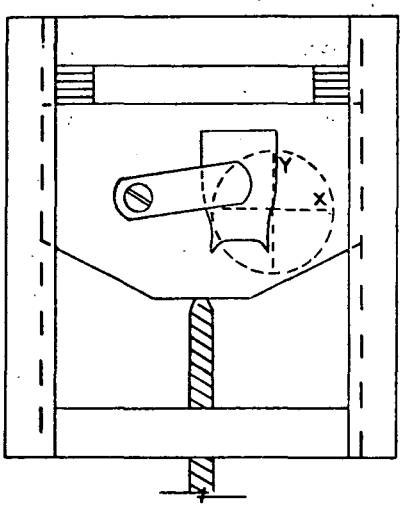

(3) SHIM AND MEASURE THE THICKNESS REDUCTION AWAY FROM FRACTURE SURFACE.

Fig. 13 Alignment Procedure of Slice Prior to Thickness Reduction Measurements

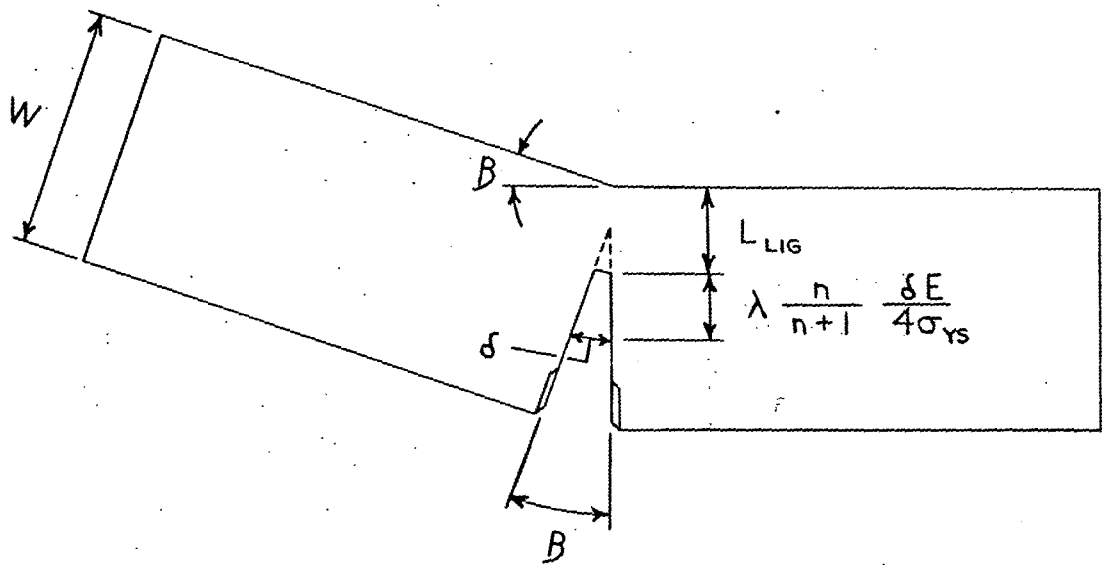

WHERE -

$$\delta = \left(\frac{L_{LIG}}{2} + \lambda \frac{n}{n+1} \frac{\delta E}{4\sigma_{YS}} \right) B$$

Fig. 14 Typical Partially Fractured Test Specimen Used in Bend Angle Procedure

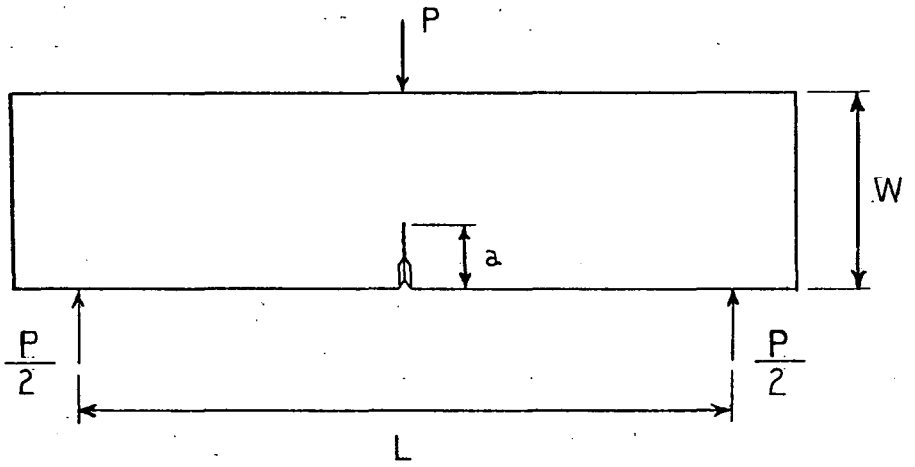

$$Y = \frac{K_C B W^2}{1.5 P L \sqrt{a}} = A_0 + A_1\left(\frac{a}{W}\right) + A_2\left(\frac{a}{W}\right)^2 + A_3\left(\frac{a}{W}\right)^3 + A_4\left(\frac{a}{W}\right)^4$$

THIS EXPRESSION WAS DEVELOPED BY GROSS AND SRAWLEY FOR SPECIMENS WHOSE L/W RATIOS ARE EITHER 8 OR 4. (ASTM STP 410)

L/W	A_0	A_1	A_2	A_3	A_4
8	+1.96	-2.75	+13.66	-23.98	+25.22
4	+1.93	-3.07	+14.53	-25.11	+25.80
3.33	+1.93	-3.12	+14.68	-25.30	+25.90

Fig. 15 K Calibration for Lehigh Test Specimen

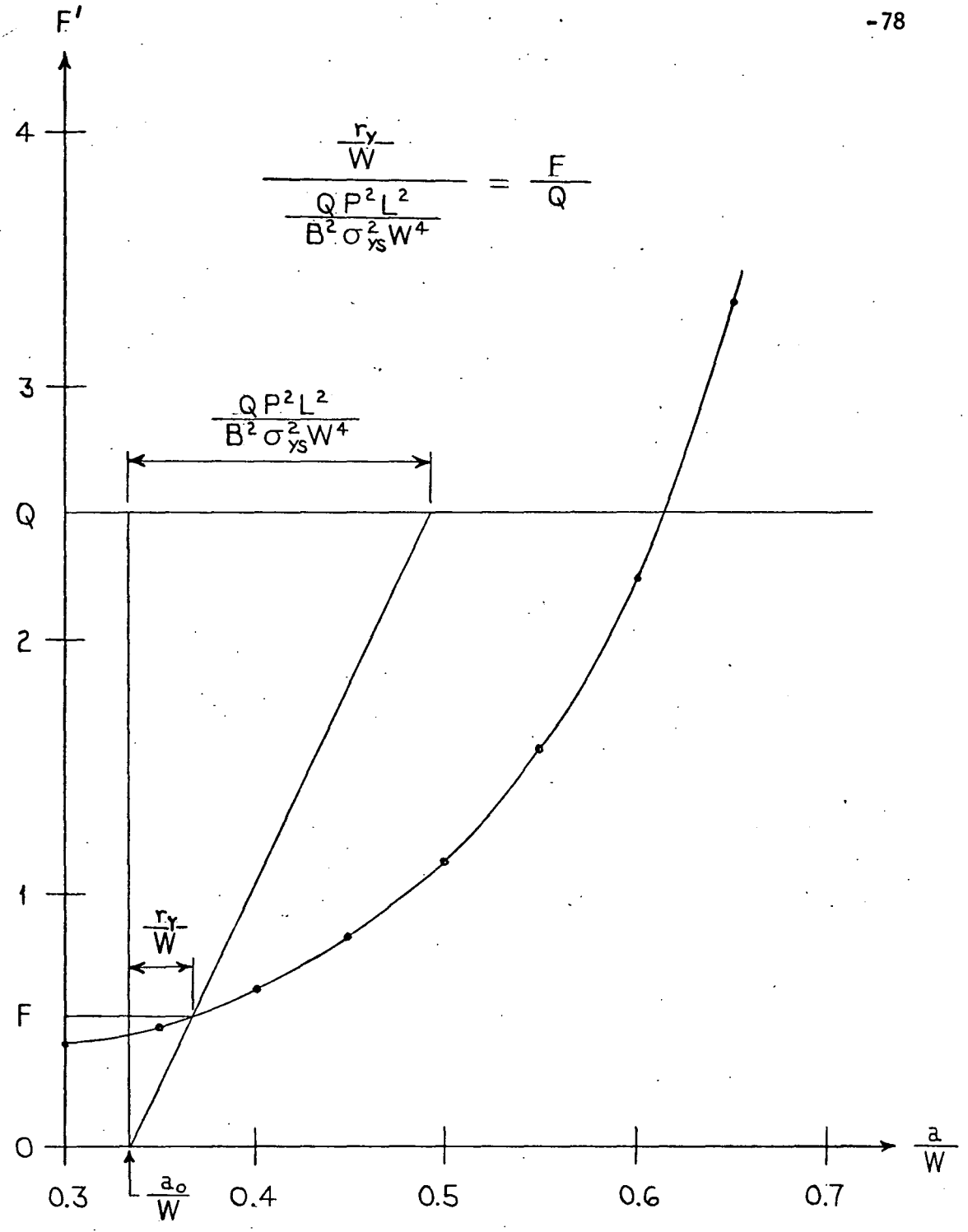

Fig. 16 Graphical Solution for K_c

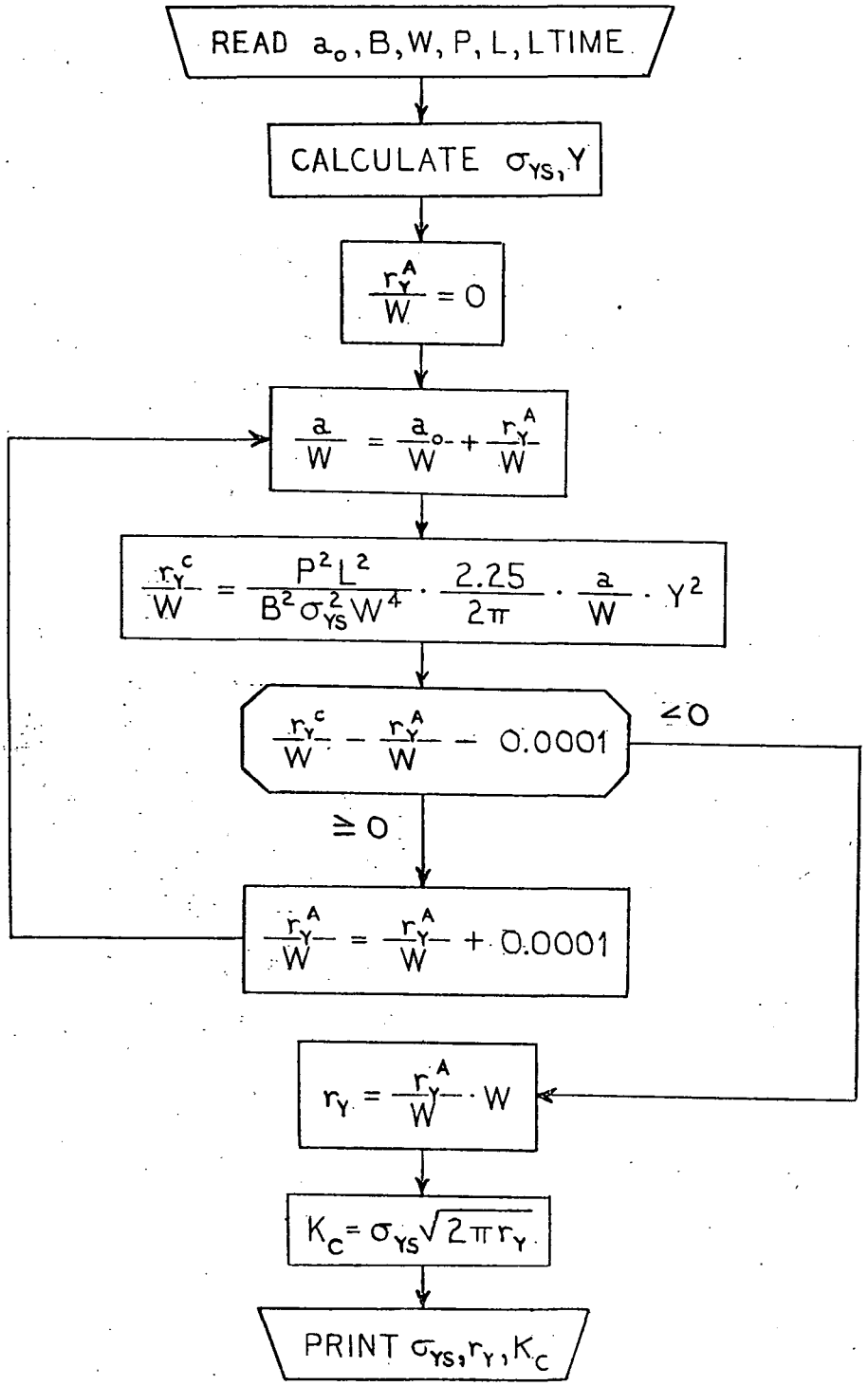

Fig. 17 Flow Chart for the Computer Solution for K_c

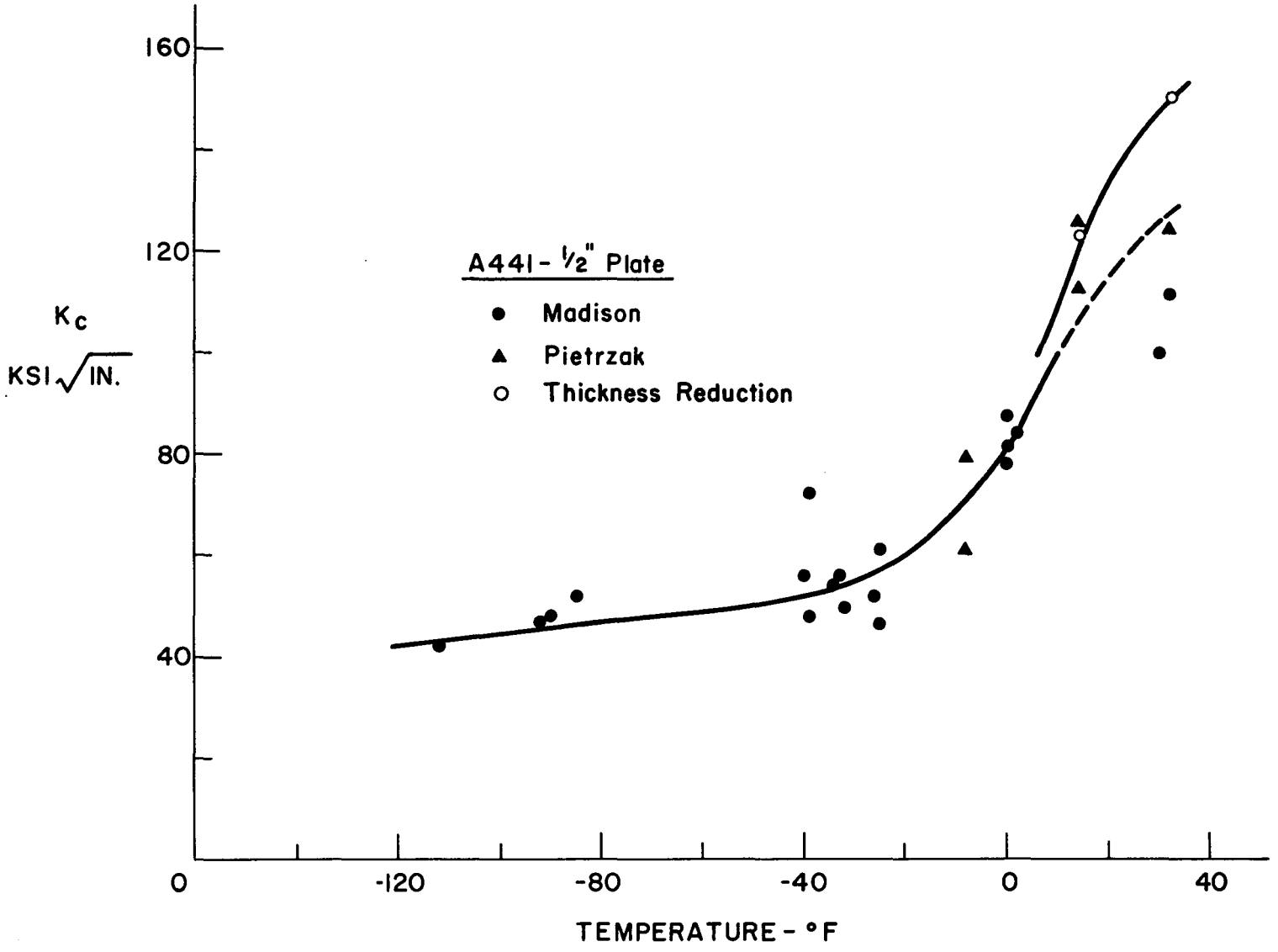

Fig. 18 K_c versus Temperature for A441 - 1/2" Plate

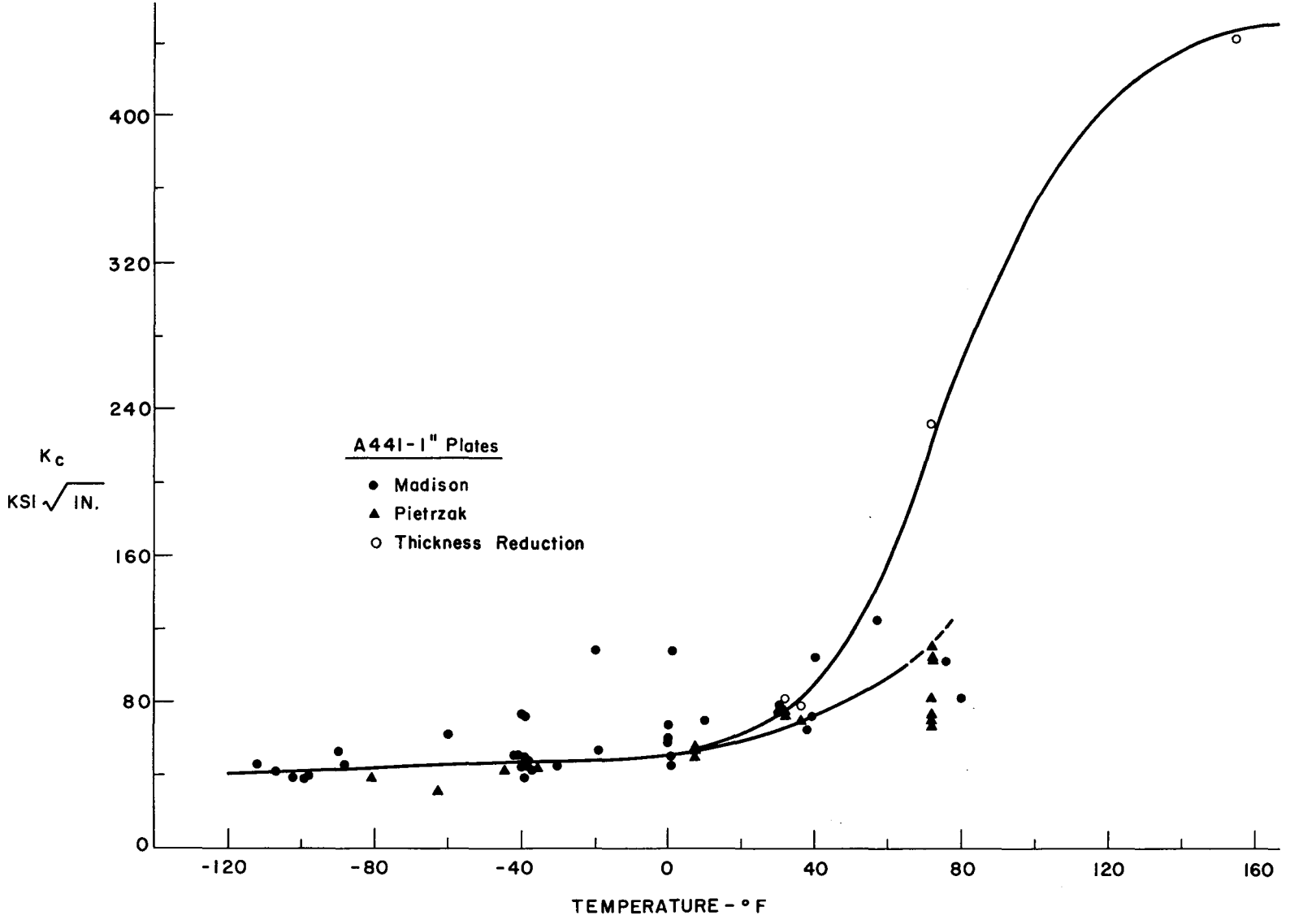

Fig. 19 K_c versus Temperature for A441 - 1" Plate

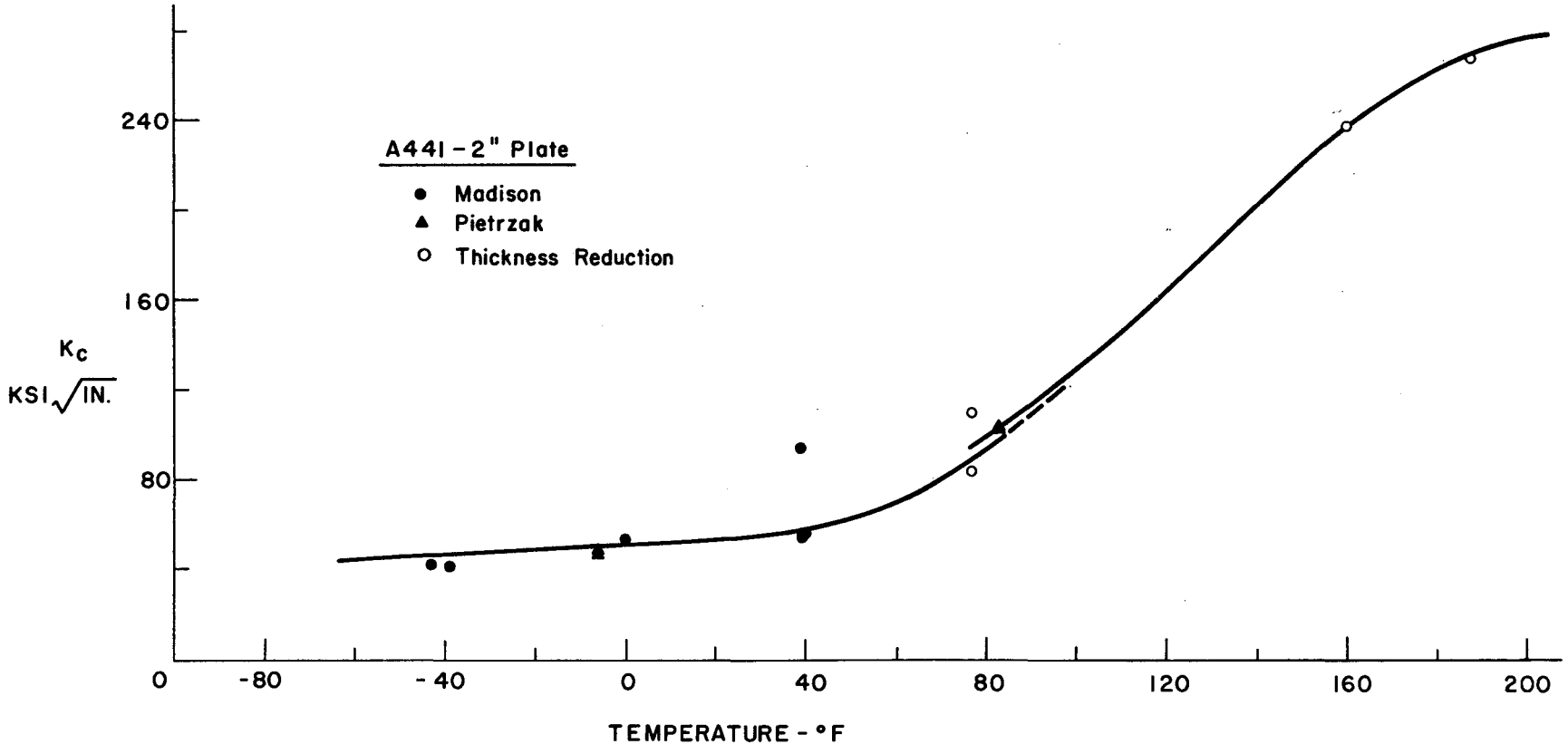

Fig. 20 K_c versus Temperature for A441 - 2" Plate

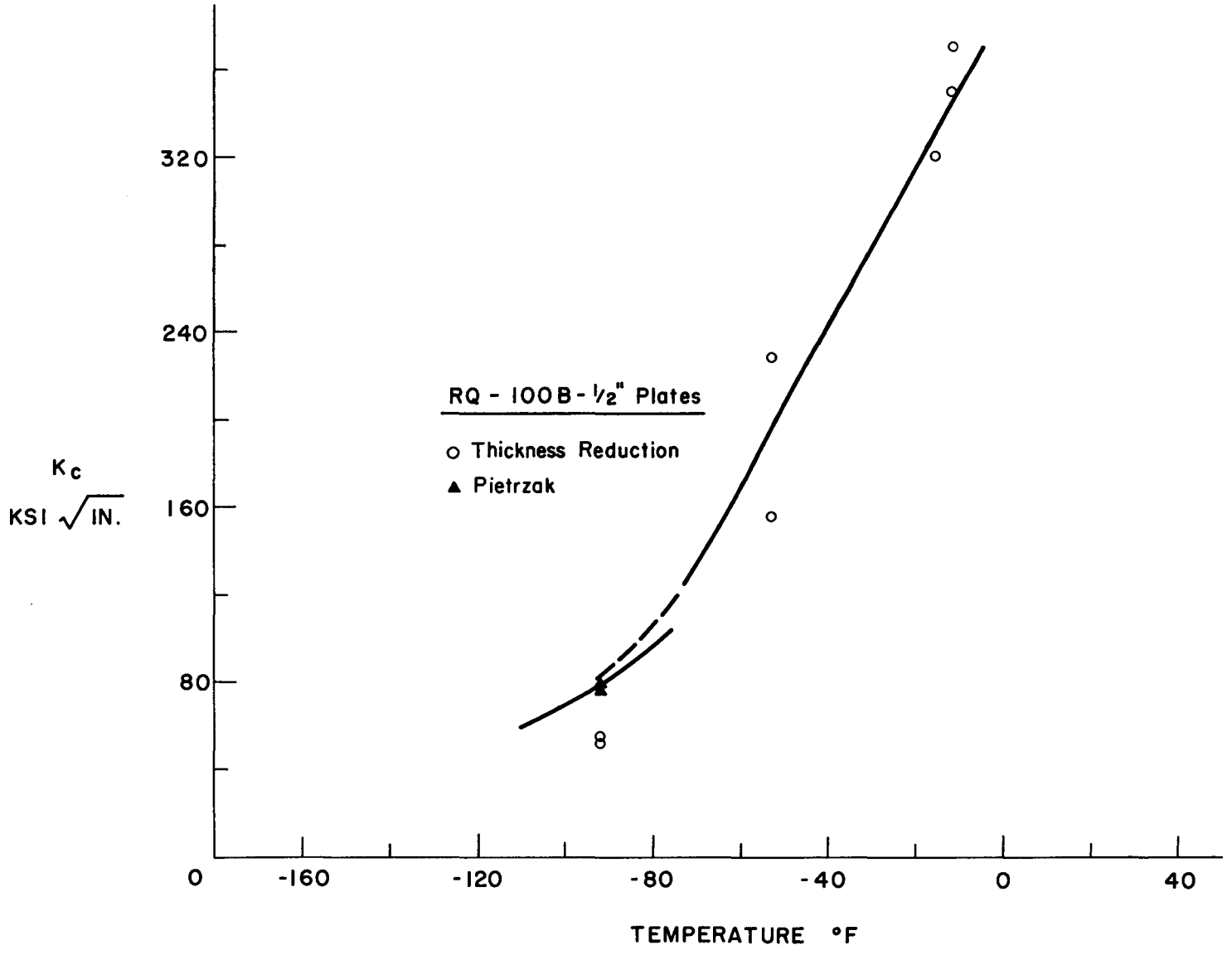

Fig. 21 K_c versus Temperature for RQ-100B - 1/2" Plate

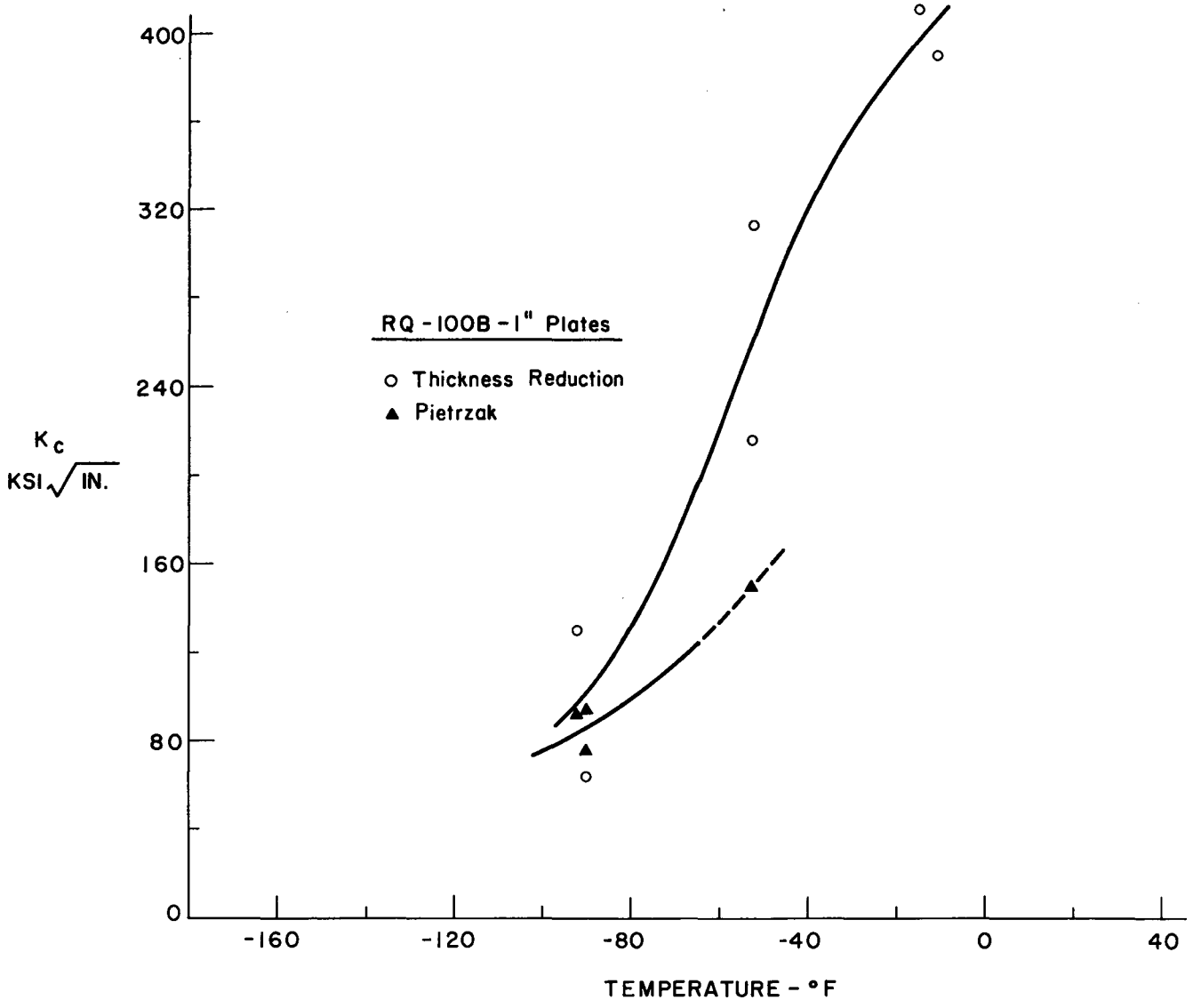

Fig. 22 K_c versus Temperature for RQ-100B - 1" Plate

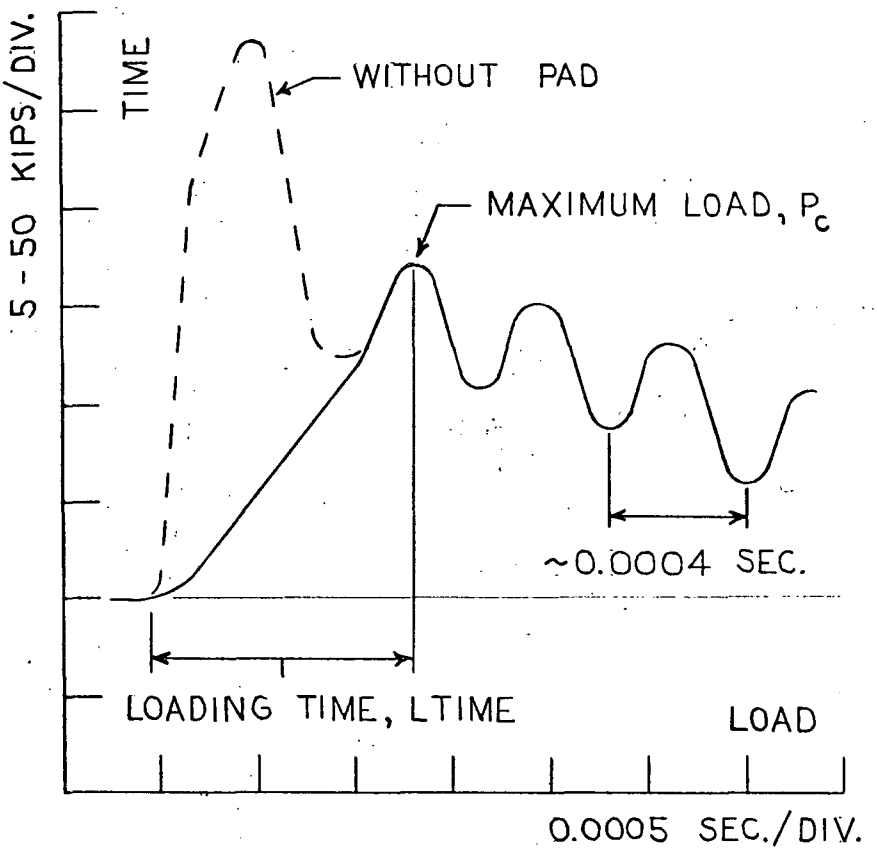

Fig. 23 Typical Load-Time Record

1.] REFLECTED WAVE MOTION

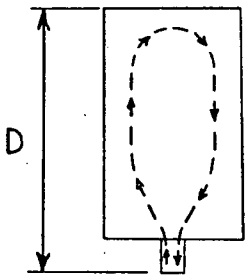

$V = \text{VELOCITY} = \sqrt{\frac{E}{\rho}}$

$T' = \text{PERIOD} = \frac{2D}{V}$

$T = 2.3 \times 10^{-4}$ SEC.

2.] BENDING WAVE MOTION

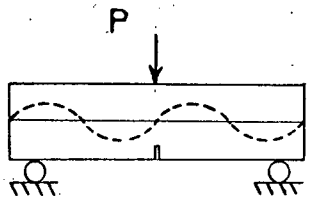

$T' = \text{PERIOD} = 2\pi \sqrt{\frac{M'}{K'}}$

WHERE $K' = \frac{1}{C}$

$T = 8.4 \times 10^{-3}$ SEC.

3.] SHEAR WAVE MOTION

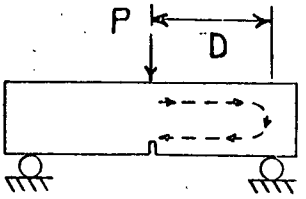

$V = \text{VELOCITY} = \sqrt{\frac{G}{\rho}}$

$T' = \text{PERIOD} = \frac{2D}{V}$

$T = 0.8 \times 10^{-4}$ SEC.

Fig. 24 Investigations into a Typical Load-Time Record Response

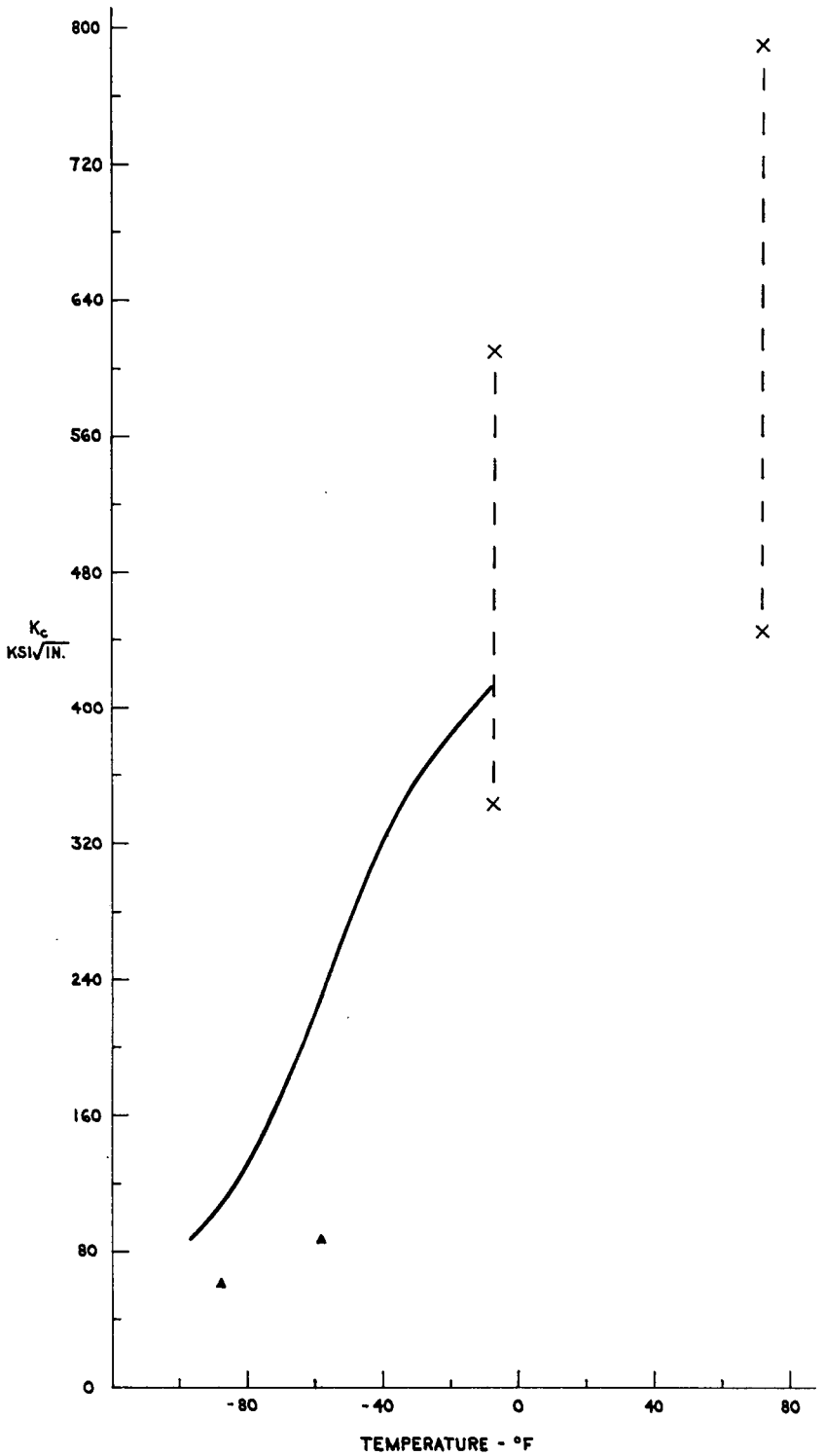

Fig. 25 Solid Curve is copied from Fig. 22 to show K_c versus Temperature Trend for RQ-100B - 1" Plate (σ_{YS} = 80 ksi). Symbols, ▲ amd X, show K_c from Maximum Load and K_c from Plastic Bend Angle for A514 - 2" Plate

REFERENCES

1. Irwin, G. R.
   ANALYSIS OF STRESSES AND STRAINS NEAR THE END OF A CRACK TRANSVERSING A PLATE, Trans. ASME, Journal of Applied Mechanics, Vol. 24, 1957, p. 361

2. Irwin, G. R.
   PLASTIC ZONE NEAR A CRACK AND FRACTURE TOUGHNESS, 7th Sagamore Ordnance Materials Research Conference, Proc. published by Syracuse University, 1961

3. Madison, R. B.
   APPLICATION OF FRACTURE MECHANICS TO BRIDGES, Fritz Engineering Laboratory Report No. 335.2, Lehigh University, 1969

4. Luft, D. E., Madison, R. B. and Irwin, G. R.
   MEASUREMENT OF DYNAMIC K_c FROM THE DEOP-WEIGHT TEAR TEST, Fritz Engineering Laboratory Report No. 335.1, Lehigh University, 1968

5. Brown, Jr., W. F. and Srawley, J. E.
   PLANE STRAIN CRACK TOUGHNESS TESTING OF HIGH STRENGTH METALLIC MATERIALS, ASTM STP410, Philadelphia, Pa., 1966

6. Irwin, G. R., Lingaraju, B. and Tada, H.
   INTERPRETATION OF THE CRACK OPENING DISLOCATION CONCEPT, Fritz Engineering Laboratory Report No. 358.2, Lehigh University, 1969

7. Srawley, J. E. and Brown, Jr., W. F.
   FRACTURE TOUGHNESS TESTING METHOD, Fracture Toughness Testing and its Application, ASTM STP381, 1965

8. Gross, B. and Srawley, J. E.
   STRESS INTENSITY FACTORS FOR THREE-POINT BEND SPECIMEN BY BOUNDARY COLLOCATION, Technical Note D-3092, NASA, December 1965

9. Irwin, G. R.
   LINEAR FRACTURE MECHANICS, FRACTURE TRANSITION AND FRACTURE CONTROL, Journal of Engineering Fracture Mechanics, Vol. 1, No. 2, 1968.

VITA

Kenneth James Pietrzak was born April 1, 1947 in Brooklyn, New York to Mr. and Mrs. Roman S. Pietrzak. He attended S. S. Cyril and Methodius School in Brooklyn, New York, where he graduated in June 1960. His high school education was completed at Bishop Loughlin Memorial High School, Brooklyn, New York, from which he graduated in June 1964.

From 1964 to 1968 he attended Manhattan College, Bronx, New York. He completed his undergraduate requirements in June 1968 and graduated with a Bachelor of Science in Civil Engineering, majoring in Structural Engineering. He worked at Gibbs and Cox, Inc., New York, New York, a naval architectural firm, as an assistant design engineer from 1968 to 1969.

In June 1969 he married MaryJane Parillo of Waterbury, Connecticut. He started his program for a Master of Science in Civil Engineering at Lehigh University, Bethlehem, Pennsylvania, in July 1969 and graduated in June 1971. His major is Structural Engineering.